A new species of mixosaurid ichthyosaur from the Middle Triassic of Luxi County, Yunnan Province, South China

YE-WEI FANG, ANDRZEJ S. WOLNIEWICZ, and JUN LIU

Fang, Y.-W., Wolniewicz, A.S., and Liu, J. 2024. A new species of mixosaurid ichthyosaur from the Middle Triassic of Luxi County, Yunnan Province, South China. *Acta Palaeontologica Polonica* 69 (2): 263–280.

Ichthyosaurs, an iconic lineage of Mesozoic marine reptiles, were an important component of recovering ecosystems after the Permo-Triassic Mass Extinction event. Mixosauridae, a clade of small, early-diverging ichthyosaurs, were of particular significance for this process, being abundant predators in Middle Triassic shallow seas. Despite the abundance of well-preserved mixosaurid specimens from South China, *Mixosaurus panxianensis* remains the only comprehensively described species, hindering our understanding of the variability, taxonomy and diversity of mixosaurids from this region. Here, we report a new species of *Mixosaurus*, *Mixosaurus luxiensis*, from Luxi County, Yunnan Province, South China. The wider postorbital skull portion differentiates the new species from *Mixosaurus cornalianus* and *Mixosaurus kuhnschnyderi* from central Europe. The non-durophagous dentition, composed of tiny piercing mesial teeth and robust but pointed distal teeth, resembles the dentition of *M. cornalianus*. However, the distal teeth of *M. luxiensis* sp. nov. are twice the size of the mesial ones, in contrast to *M. cornalianus*, in which the mesial and distal teeth are approximately equal in size. The forelimb exhibits a unique morphology, including a proportionally narrow radius, the presence of a peripheral notch on the ulna, and a large metacarpal V. A preliminary phylogenetic analysis suggests a close affinity of the new taxon with *M. cornalianus* from Western Tethys. Our study introduces important, new anatomical information on *Mixosaurus* from South China, useful for future studies of mixosaurid diversity.

Key words: Ichthyosauria, Mixosauridae, marine reptile, phylogeny, biotic recovery, Guanling Formation, Anisian, Triassic.

Ye-Wei Fang [paleofang@gmail.com; ORCID: https://orcid.org/0000-0002-8150-6331] and Jun Liu [junliu@hfut.edu.cn; ORCID: https://orcid.org/0000-0001-7859-5209] (corresponding author), School of Resources and Environmental Engineering, Hefei University of Technology, 193 Tunxi Road, Hefei 230009, Anhui, China.
Andrzej S. Wolniewicz [asw49@cam.ac.uk; ORCID: https://orcid.org/0000-0002-6336-8916], School of Resources and Environmental Engineering, Hefei University of Technology, 193 Tunxi Road, Hefei 230009, Anhui, China; Department of Earth Sciences, University of Cambridge, Downing Street, Cambridge, CB2 3EQ, UK; Institute of Paleobiology, Polish Academy of Sciences, Twarda 51/55, 00-818 Warsaw, Poland.

Received 8 January 2024, accepted 10 April 2024, published online 14 June 2024.

Introduction

The Permo-Triassic Mass Extinction (PTME) was the most severe extinction event in the Phanerozoic (Bambach 2006). Despite its devastating effect on biodiversity, Triassic ecosystems recovered within only a few million years after the PTME (Brayard et al. 2017; Dai et al. 2023). The richness of benthic communities increased rapidly in the early Middle Triassic (Anisian) and stabilized towards its end (Chen and Benton 2012; Friesenbichler et al. 2021), while pelagic ecosystems perhaps regenerated even earlier (Song et al. 2018; Qiao et al. 2022). Mesozoic marine reptiles, such as ichthyosaurs and sauropterygians, colonized the marine realm in the aftermath of the PTME and quickly became important predators in Triassic seas (Carroll 1997; Fröbisch et al. 2013; Liu et al. 2014; Li and Liu 2020; Sander et al. 2021). Because predators are important indicators of ecosystem complexity, obtaining a detailed knowledge of their taxonomic and ecological diversity throughout the Triassic is important for understanding the process of marine ecosystem recovery after the PTME (Benton et al. 2013; Scheyer et al. 2014; Motani et al. 2015; Liu and Sander 2019).

Ichthyosaurs were one of the most successful groups of Mesozoic marine reptiles (Motani 2005a; Bardet et al. 2014). The earliest ichthyosaur fossils are known from the Early Triassic, but it is unclear if the clade originated in the latest Permian or earliest Triassic (Motani et al. 2017; Kear et al. 2023). Ichthyosaurs achieved a broad geographic distribu-

tion and high ecological diversity by the Middle Triassic (Callaway 1989; Sander and Mazin 1993; McGowan and Motani 2003; Liu 2011). Mixosauridae was a short-lived, but abundant clade of ichthyosaurs from the Middle Triassic. They evolved a fusiform body plan and had powerful jaw muscles (Motani et al. 1996; Maisch and Matzke 2000; McGowan and Motani 2003; Renesto et al. 2020). Their fossils are known mainly from shallow water sediments, like the Muschelkalk in Germany and Poland (Maisch and Matzke 1998a), the Besano Formation in Italy/Switzerland (Brinkmann 1997; Renesto et al. 2020), the Vega-Phroso siltstone and the Llama members of the Sulphur Mountain Formation in Canada (Callaway and Brinkman 1989), and the Upper Member of the Guanling Formation in South China (Benton et al. 2013; Liu et al. 2013), but they are also found in more pelagic sediments, such as the Botneheia Formation in Spitsbergen (Maxwell and Kear 2013; Hurum et al. 2014) and the Fossil Hill Member of the Favret Formation in the western United States (Schmitz et al. 2004; Sander et al. 2021). Mixosaurids have a long history of research, dating back to the 19th century (Quenstedt 1852; Hulke 1873; Bassani 1886; Baur 1887) and are one of the better-known ichthyosaur groups. Their anatomy (Callaway 1997; Motani 1999b; Brinkmann 2004), histology (Kolb et al. 2011), reproduction (Brinkmann 1996; Miedema et al. 2023b), ontogeny (Kolb et al. 2011; Miedema et al. 2023a), intraspecific variation (Maisch and Matzke 1998b; Zhou et al. 2022), and even body outline (Renesto et al. 2020) have all been studied in detail.

The monophyly of Mixosauridae is well-established and supported by several synapomorphies of the circumnarial area, skull roof, girdles, limbs, and vertebrae (Liu 2011; Ji et al. 2016; Moon 2019). However, the taxonomy of Mixosauridae remains incompletely understood. Mixosauridae are traditionally divided into two genera, *Mixosaurus* and *Phalarodon*, which differ from each other in narial shelf, dentition, humerus and caudal centrum morphology (Schmitz et al. 2004; Schmitz 2005; Jiang et al. 2006; Liu et al. 2013). Nonetheless, the taxonomic composition and phylogenetic topology within these genera differ between studies. Whereas the majority of ichthyosaur researchers follow the *Mixosaurus–Phalarodon* dichotomy (Jiang et al. 2006; Ji et al. 2016; Motani et al. 2017; Økland et al. 2018; Huang et al. 2019; Roberts et al. 2022), Maisch (2010) and Moon (2019) separated *Mixosaurus panxianensis* and *Phalarodon atavus* into distinct genera (*Barracudasauroides* and *Contectopalatus*, respectively). In addition, some phylogenetic analyses have failed to recover Mixosauridae resolved into a simple *Mixosaurus–Phalarodon* dichotomy (Liu 2011; Huang et al. 2019; Moon 2019). Therefore, it is possible that the taxonomy and phylogeny of mixosaurids are more complex than the current paradigm suggests.

Over the past 20 years, abundant fossils of mixosaurids have been recovered from the Middle Triassic strata of South China (Motani et al. 2008; Jiang et al. 2009; Hu et al. 2011). Despite the abundance of fossils, the taxonomic composition of mixosaurids from South China remains only partly known. A total of six species of *Mixosaurus* has been erected based on Chinese materials ("*Mixosaurus maotaiensis*" from Renhuai City, early Anisian [Young 1965], "*Mixosaurus guanlingensis*" from Guanling biota, early Carnian [Yin et al. 2000], *Mixosaurus panxianensis* from Panxian fauna, Pelsonian, Anisian [Jiang et al. 2005, 2006], "*Mixosaurus yangjuanensis*" from Panxian fauna [Liu and Yin 2008], "*Mixosaurus xindianensis*" from Panxian fauna [Chen and Cheng 2010], and "*Mixosaurus xinzhaiensis*" from Luoping biota, Pelsonian, Anisian [Chen et al. 2016]). In addition, the occurrence of four additional mixosaurid species, known from Europe and the USA, was also reported from South China (*Phalarodon* cf. *P. fraasi* from Panxian fauna [Jiang et al. 2007], *Phalarodon atavus* from Luoping biota [Liu et al. 2013], "*Mixosaurus cornalianus*" from Panxian fauna [Liu and Yin 2008], and "*Mixosaurus kuhnschnyderi*" from Luoping biota [Chen and Cheng 2009]). Furthermore, three mixosaurid specimens, referable only to family or genus level, were also described from South China (*Phalarodon* sp. from Panxian fauna [Jiang et al. 2003], Mixosauridae gen. et sp. indet. from Luoping biota [Liu et al. 2011], *Mixosaurus* sp. from Fuyuan County, upper Ladinian [Chen et al. 2016]), but it is not clear whether these specimens represent new taxa or are referable to any of the currently known mixosaurid species.

However, three of the *Mixosaurus* species reported from South China ("*M. maotaiensis*", "*M. guanlingensis*", and "*M. yangjuanensis*"), and one occurrence of an otherwise European taxon ("*M. cornalianus*"), were subsequently identified as invalid (McGowan and Motani 2003; Jiang et al. 2006, 2007, 2008a). Among the remaining species new to South China, "*M. xindianensis*" and "*M. xinzhaiensis*" were inadequately figured and only briefly described (due to inaccessibility of the holotype for study, the former was even regarded as species inquirendae by Liu et al. 2013). As a consequence, *Mixosaurus panxianensis* is the only species of *Mixosaurus* from South China that has been comprehensively described and well-illustrated (Jiang et al. 2005, 2006), but whether it represents a species of *Mixosaurus* (Jiang et al. 2006; Ji et al. 2016) or a separate genus (Maisch 2010; Moon 2019) remains a matter of debate. Incomplete knowledge of the anatomy and taxonomy of *Mixosaurus* species from South China hinders our understanding of the global diversity, phylogenetic interrelationships, and palaeobiogeography of mixosaurids.

Here, we report a new species of *Mixosaurus* collected from a recently discovered shallow marine fauna in Luxi County, Yunnan Province, South China (Wen et al. 2020; Xu et al. 2022; Hu and Liu 2023; Lu and Liu 2023; Hu et al. 2024) (see Fig. 1 for localities of the eosauropterygians Nothosauroidea indet. (Hu and Liu 2023) and *Dianmeisaurus mutaensis* near Muta (Hu et al. 2024) and the tanystropheid *Luxisaurus terrestris* near Suomeiluo (Lu and Liu 2024). An anatomical description of the new species is provided,

highlighting the most important differences and similarities with other species of *Mixosaurus*. A preliminary phylogenetic analysis of mixosaurid interrelationships, incorporating anatomical information from the new species, is also presented and discussed.

Institutional abbreviations.—CCCGS, Chengdu Center of China Geological Survey, China; GMPKU, Geological Museum of Peking University, Beijing, China; HFUT, Geological Museum of Hefei University of Technology, China; PIMUZ, Department of Palaeontology, University of Zürich, Switzerland (formerly Paläontologisches Institut und Museum der Universität Zürich, Switzerland); PMU, Paleontological Museum, University of Uppsala, Sweden; SMNS, Staatliches Museum für Naturkunde Stuttgart, Germany; YIGMR, Yichang Institute of Geology and Mineral Resources (currently WCCGS, Wuhan Center of China Geological Survey), China.

Nomenclatural acts.—This published work and the nomenclatural acts it contains have been registered in ZooBank: urn:lsid:zoobank.org:act:AF9FF8CE-A718-48E3-9132-A11FA3392666

Material and methods

HFUT HL-21-08-002 was collected from a quarry about one kilometer southeast of Huale Village, Luxi County, Yunnan Province, China (Fig. 1). It originates from the Upper Member (also known as Second Member or Member II) of the Guanling Formation (formerly part of the Gejiu Formation) and is Pelsonian (middle Anisian) in age (Wen et al. 2020; Xu et al. 2022; Hu and Liu 2023; Lu and Liu 2023; Hu et al. 2024), similar to the Luoping and Panxian faunas located nearby (Benton et al. 2013). The rock matrix of thinly lam-

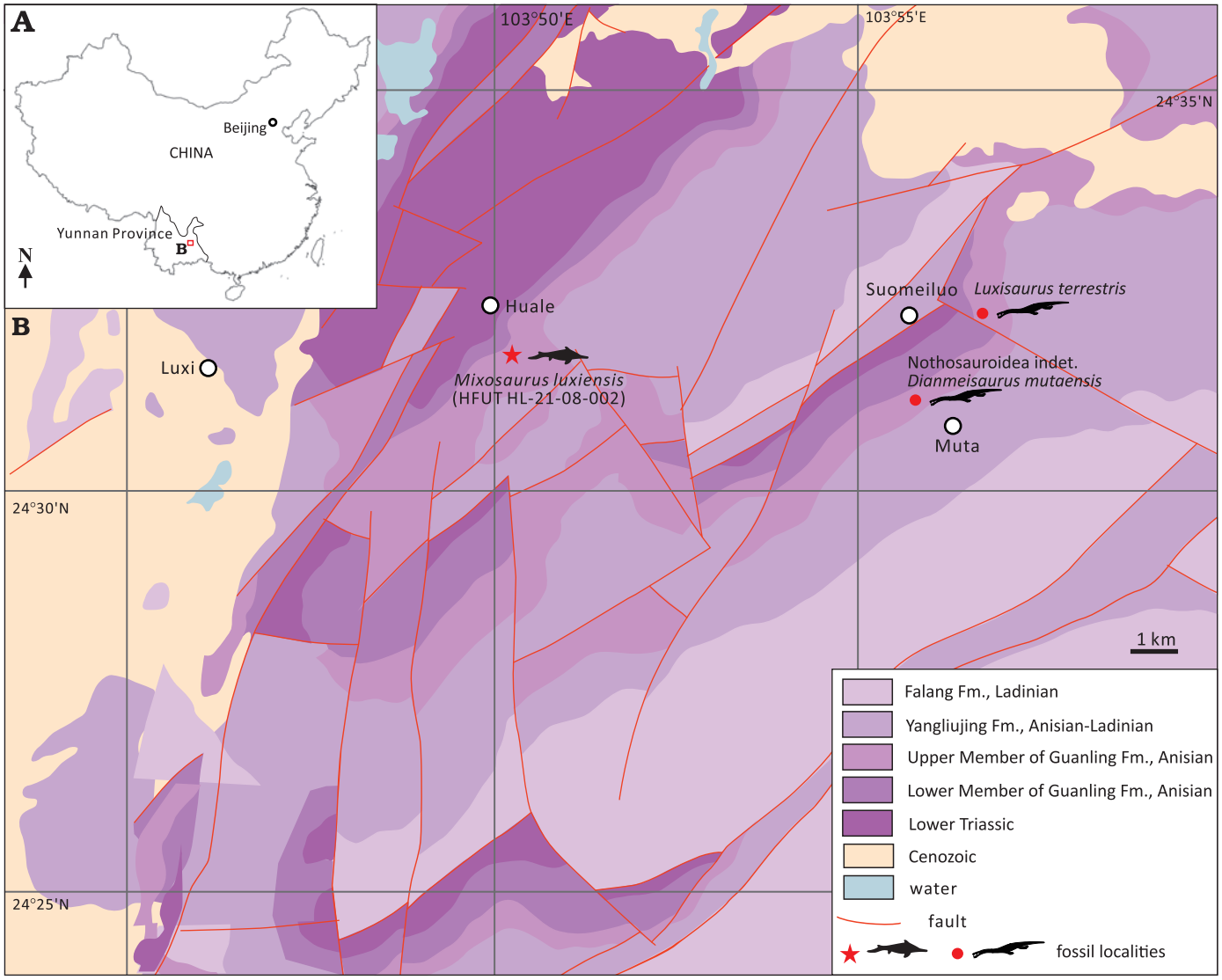

Fig. 1. **A**. Map of China showing location of the study area. **B**. The geological map of the area around Luxi, Yunnan Province, South China, showing the locality of HFUT HL-21-08-002 (modified after Hu and Liu 2022; Lu and Liu 2023; Hu et al. 2024). Abbreviation: Fm., Formation.

inated micritc limestone with alternating interlayers indicates an intraplatform sedimentary facies, similar to the depositional setting of the Luoping Biota (Hu et al. 2011; Wen et al. 2020).

HFUT HL-21-08-002 is accessioned in the collections of the Geological Museum of Hefei University of Technology in Hefei, Anhui Province, China (HFUT). It was prepared using mounted needles and pneumatic tools in the paleontological preparation laboratory of HFUT. Detailed observations of the specimen were taken under a LEICA S9i microscope. Canon EOS 80D and Nikon D7200 cameras with macro lenses were used for specimen photography.

The phylogenetic analysis was based on a recently published, comprehensive data matrix for ichthyosaurs (Huang et al. 2019). HFUT HL-21-08-002 was added to this character-taxon matrix. Characters 43(?), 50(?), 51(?), 175(?), 187(?) were re-coded for *M. cornalianus* to 43(0), 50(0), 51(0), 75(0), 187(0) (based on Miedema et al. 2023a). Character 43 was re-coded for *M. kuhnschnyderi* from 43(?) to 43(0) (based on PIMUZ T 1324; Brinkmann 2004). Character 112 was re-coded for *M. panxianensis* from 112(1) to 112(0) (based on GMPKU-P-1008 and GMPKU-P-1038 [holotype]; Jiang et al. 2005, 2006), for *M. cornalianus* from 112(1) to 112(0&1) (based on figures in Maisch and Matzke 1998b, Motani 1999a, Renesto et al. 2020, and Zhou et al. 2022), and for *M. kuhnschnyderi* from 112(1) to 112(?) (based on PIMUZ T 1324; Brinkmann 2004). The phylogenetic matrix (SOM 2, Supplementary Online Material available at http://app.pan.pl/SOM/app68-Fang_etal_SOM.pdf) was edited in Mesquite 3.81 (Maddison and Maddison 2023) and analyzed in TNT 1.5 (Goloboff and Catalano 2016). All characters were treated as unordered and equally weighted. Max. trees was set to 10 000. Collapsing was set to "max. length = 0", using rule 3-collapse. Traditional Search using 1000 Wagner tree replications was applied to obtain maximum parsimony trees. The Bremer support values were calculated using TBR branch-swapping from existing trees, retaining trees suboptimal by 100 steps. Iterative Positional Congruence Reduced (IterPCR) was used to prune unstable taxa in a second analysis, in order to obtain a better-resolved reduced strict consensus cladogram (Pol and Escapa 2009).

Systematic palaeontology

Ichthyosauria de Blainville, 1835

Mixosauridae Baur, 1887

Genus *Mixosaurus* Baur, 1887

Type species: *Mixosaurus cornalianus* Bassani, 1886; Monte San Giorgio, Italy and Switzerland; late Anisian–early Ladinian, Middle Triassic.

Emended diagnosis (modified after Brinkmann 2004; Jiang et al. 2006; Liu 2011; Ji et al. 2016; and Renesto et al. 2020).—Centrum height/length ratio moderately increased in the mid-caudal region, but not exceeding a value of 3.0 (centrum height/length index significantly increased in the mid-caudal region to a value of over 3.0 in *Phalarodon*); interclavicle T-shaped with transversal bars perpendicular to the posterior process (interclavicle V-shaped, with posterior process triangular and broad, and transversal bars triangular, narrow and projecting anterolaterally in *Phalarodon*); humerus relatively broad with proximodistal length subequal to anteroposterior width (humerus narrow, proximodistally longer than anteroposteriorly wide in *Phalarodon*).

Mixosaurus luxiensis sp. nov.

Figs. 2–7; SOM 1: figs. S1, S2, tables S1, S2.

ZooBank LSID: urn:lsid:zoobank.org:act:AF9FF8CE-A718-48E3-9132-A11FA3392666

Etymology: In reference to the type locality in Luxi County.

Holotype: HFUT HL-21-08-002, a nearly complete skeleton, with the postcranium mostly disarticulated.

Type locality: Huale Village, Luxi County, Yunnan Province, China.

Type horizon: Upper (Second) Member of the Guanling Formation, Pelsonian, Anisian, Middle Triassic.

Diagnosis.—A species of *Mixosaurus* characterised by the following combination of character states: anterior terrace of supratemporal fenestra reaching only the most posterior part of nasal (anterior terrace reaches the level of the external naris in *M. panxianensis*, *M. cornalianus*, and *M. kuhnschnyderi*); postorbital broad and postorbital portion of the skull around half the length of the orbit (similar to *M. panxianensis* and "*M. xindianensis*", proportionally longer than in *M. cornalianus* and *M. kuhnschnyderi*); jugal without posteroventral process (variable in *M. panxianensis*, absent in *M. cornalianus*); no distinct plicidentine (also absent in *M. cornalianus*, present in *M. panxianensis*); anterior teeth slender and remarkably small (similar to *M. cornalianus*, different from *M. panxianensis* and *M. kuhnschnyderi*, in which the anterior dentition is relatively larger); dentition weakly heterodontous, posterior teeth robust but pointed (similar to *M. cornalianus*, different from "*M. xindianensis*", *M. panxianensis*, and *M. kuhnschnyderi*, in which the posterior teeth are molariform and mesiodistally elongated); centrum height/length ratio varying from <1.5 (anterior dorsal) to 2.0 (postflexural caudal) (up to 2.0 for *M. cornalianus* [Schmitz et al. 2004; Schmitz 2005], higher than 2.0 in *M. panxianensis* [Zang 2014], *M. kuhnschnyderi* [Brinkmann 2004], and "*M. xindianensis*" [Chen and Cheng 2010]); radius narrow (proximodistal length/midshaft width ratio = 2.4; 1.5–1.9 for *M. panxianensis* and *M. cornalianus*), carrying two notches on the leading edge (present in *M. panxianensis*, variable in *M. cornalianus*, absent in *M. kuhnschnyderi* and "*M. xindianensis*"); single notch on the posterior margin of the ulna (present in "*M. xindianensis*", rarely occurring in *M. panxianensis*, absent in *M. cornalianus*, *M. kuhnschnyderi*, and "*M. xinzhaiensis*"); metacarpal V larger in size than distal carpal IV and probably bearing a notch (small and without notch in other *Mixosaurus* species, but similar in size and morphology to the Luoping specimen of *Phalarodon atavus* [Liu et al. 2013]); proximal phalanges in digit 1 well-emarginated at the leading edge of the forefin

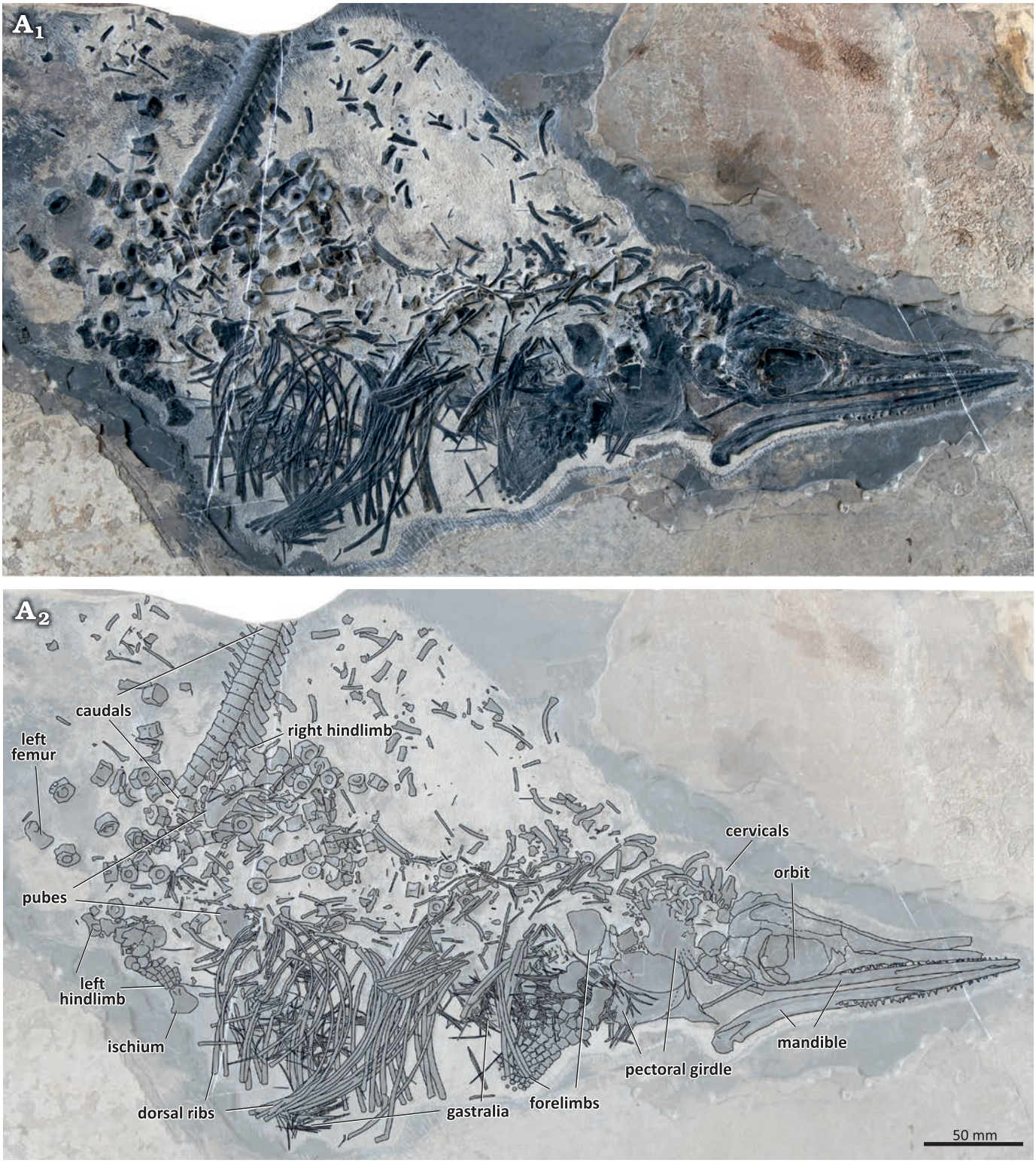

Fig. 2. The holotype of the mixosaurid ichthyosaur *Mixosaurus luxiensis* sp. nov. (HFUT HL-21-08-002) from Huale Village, Luxi County, Yunnan Province, China (Pelsonian, Anisian). Photograph (A_1) and interpretative drawing (A_2). Dashed lines indicate inferred margins.

(anterior margin complete in *M. cornalianus*, also emarginated in *M. panxianensis* and "*M. xinzhaiensis*"). Except for displaying the diagnostic features of *Mixosaurus*, HFUT HL-21-08-002 possesses the following character states inconsistent with a referral to *Phalarodon*: narial shelf and buccal ridge absent; dental groove present posteriorly; dentary labial shelf absent; plicidentine absent.

Description.—HFUT HL-21-08-002 comprises an almost complete, partially articulated skeleton exposed in right lateral view, with only the posterior caudals missing (Fig. 2).

The humeral head of HFUT HL-21-08-002 is not convex and evident striations are present on its surface. On the other hand, the basioccipital has a midline ridge and lateral bulges developed, and lacks a ventral invagination. These features indicate the specimen likely represents an advanced juvenile or osteologically immature adult (Liu 2011; Liu et al. 2013; Miedema et al. 2023a). The estimated total length of HFUT HL-21-08-002 is around 75 cm (based on the mandibular length, following the formula provided by Brinkmann 2004), making *M. luxiensis* sp. nov. one of the smallest known mixosaurids, comparable in size to *M. kuhnschnyderi* (Brinkmann 1998b, 2004). The mandible of HFUT HL-21-08-002 (160 mm in length) is about the same length as that of the holotype of *M. kuhnschnyderi* (PIMUZ T 1324) (mandible length 164 mm; Brinkmann 1998b), but its basioccipital and appendicular elements are larger than those of PIMUZ T 1324 (basioccipital length 15 mm vs. 12.5 mm; basioccipital width 12.6 mm vs. 11 mm; scapular length 46 mm vs. 40 mm; coracoid length 47 mm vs. 32 mm; humerus length 24.1 mm vs. 20.5 mm; radius length 19.9 mm vs. 15.6 mm) (Brinkmann 1998a, 2004).

Skull: The skull is mediolaterally compressed and exposed from its right lateral aspect (Fig. 3). However, because the skull was separated into two contralateral halves, the medial surfaces of the left part of the snout and the left skull roof can be seen exposed above the right side of the skull. Around 20 mm of the anterior tips of the premaxillae are missing. The preserved portion of the skull (length 131.2 mm, height 45.0 mm) is shorter than the complete mandibular rami (length ~160 mm). The orbit (length 36.8 mm, height 25.0 mm) is approximately oval in outline, although its dorsal margin is straight. The postorbital part of the skull (cheek region) is longer than half of the orbit length (18.5 mm) and occupies 27% of the postnarial length of the skull (68.6 mm). The postorbital region of HFUT HL-21-08-002 is similar in proportions to the postorbital region of *M. panxianensis*, *P. atavus*, and *P. callawayi* (Schmitz et al. 2004; Jiang et al. 2005), but differs from the condition in *M. cornalianus* and *M. kuhnschnyderi*, in which the postorbital portion of the skull is markedly shorter (Brinkmann 2004; Schmitz et al. 2004; Renesto et al. 2020).

The premaxillae constitute most of the length of the slender snout. Posteriorly, the premaxilla wedges in between the nasal and maxilla, contributing slightly to the anteroventral margin of the external naris, a feature common in mixosaurids (Schmitz et al. 2004; Liu et al. 2011, 2013). The external naris is anteroposteriorly elongated and slit-like. It is bounded by the maxilla ventrally, whereas the nasal constitutes its whole dorsal margin. The maxilla possesses a very long anterior process, extending anteriorly nearly as far as the nasal. The slender posteroventral process of the maxilla, together with the tapering posteroventral process of the lacrimal, contacts the jugal at the level of the anterior margin of the orbit. The postnarial process of the maxilla, which is slightly damaged, contacts the prefrontal and separates the external naris from the lacrimal and prefrontal. Some mixosaurids have large neurovascular foramina on the external surface of the maxilla (Maisch and Matzke 2001; Brinkmann 2004; Schmitz et al. 2004; Jiang et al. 2005), but in HFUT HL-21-08-002 these foramina seem to be absent.

The lacrimal comprises the anteroventral margin of the orbit and contacts the prefrontal dorsally, forming prominent, dorsal extensions. A pronounced antorbital ridge extends from the anterodorsal to the posteroventral part of the lacrimal. The prefrontal produces several projections anteroventrally, which interlock with the corresponding projections of the lacrimal, forming a serrate suture. The narrow posterior part of the prefrontal comprises the anterior part of the dorsal margin of the orbit, whereas the extensive anterior portion contacts the nasal, lacrimal and the postnarial process of the maxilla. Posteriorly, the prefrontal seems to contact the postfrontal along an oblique suture, but because of bone surface damage, this cannot be discerned with confidence. The prominent supraorbital crest is formed by the raised dorsal margins of the prefrontal and the postfrontal. The dorsal part of the temporal region is slightly damaged, but the postfrontal seems to contact the supratemporal posteriorly, excluding the postorbital from participation in the upper temporal fenestra, like in other mixosaurids with well-preserved skulls (Motani 1999b; Maisch and Matzke 2001; Schmitz et al. 2004).

Direct observation of the anterior extent of the anterior terrace of the supratemporal fenestra on the nasal is hindered by the mediolateral compression of the skull. However, contrasting the well-preserved and convex surface of the nasal with the crushed and collapsed surface of the frontal reveals that most parts of the nasal, except for its posterodorsal corner, likely did not contribute to the anterior terrace. The sagittal crest, which forms the medial wall of the anterior terrace, is tall and anteroposteriorly elongated. It is formed by the parietal, frontal and nasal, with the frontal comprising its majority. However, because of numerous surface cracks, the sutural contacts between these bones cannot be confidently determined. Anteriorly, the sagittal crest extends to the level of the posterior end of the external naris, being shorter than the sagittal crests in species of *Phalarodon* and *M. panxianensis*, which extend beyond the anterior end of the external naris (Merriam 1910; Maisch and Matzke 1998a, 2000; Schmitz et al. 2004; Jiang et al. 2005). The sagittal crest, which is raised markedly above the supraorbital crest in lateral view, decreases in height anteriorly and forms a smooth transition with the snout, in contrast to forming an apparent terminal "step", which is present in species of *Phalarodon* (Maisch and Matzke 1998a; Schmitz et al. 2004). Posteriorly, the sagittal crest terminates at the parietal-supratemporal suture.

The supratemporal is divided into a lateral, a medial and a ventral process. It forms the posterior rim of the skull roof and the concave, posterior margin of the upper temporal fenestra. The squamosal is taller than long and possibly produces an anteroventral process, but this is difficult to confirm because the bone is severely damaged and pos-

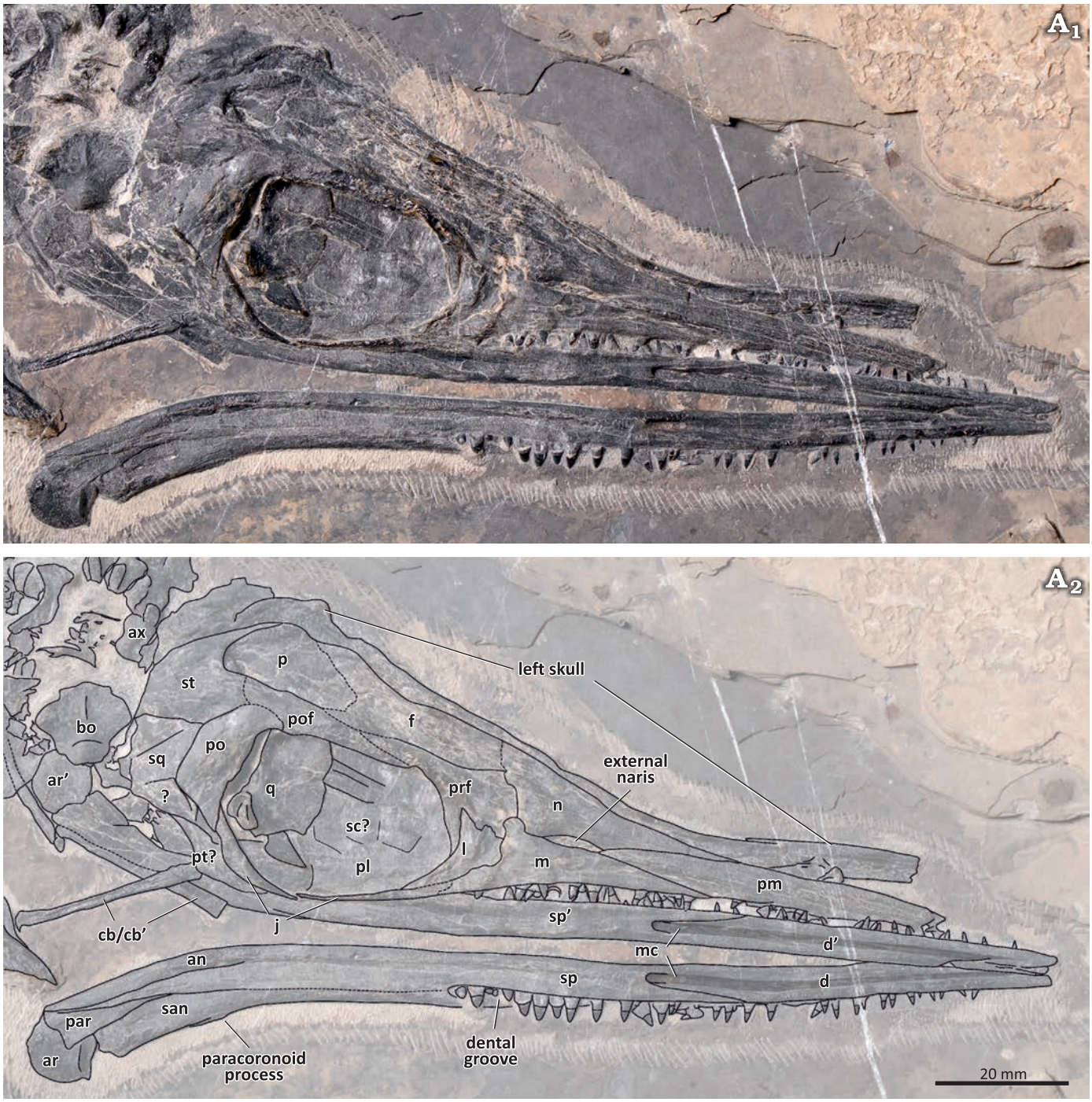

Fig. 3. The skull and lower jaw of the mixosaurid ichthyosaur *Mixosaurus luxiensis* sp. nov. (HFUT HL-21-08-002) from Huale Village, Luxi County, Yunnan Province, China (Pelsonian, Anisian). Photograph (A_1) and interpretative drawing (A_2). Dashed lines indicate inferred margins. The ' symbol indicates left elements. Abbreviations: an, angular; ar, articular; ax, axis; bo, basioccipital; cb, ceratobranchial; d, dentary; f, frontal; j, jugal; l, lacrimal; m, maxilla; mc, Meckelian canal; n, nasal; p, parietal; par, prearticular; pl, palatine; pm, premaxilla; po, postorbital; pof, postfrontal; prf, prefrontal; pt, pterygoid; q, quadrate; qj, quadratojugal; san, surangular; sc, scleral plate; sp, splenial; sq, squamosal; st, supratemporal.

sesses several surface cracks. The postorbital constitutes the posterodorsal margin of the orbit and contacts the adjacent supratemporal, postfrontal, squamosal, and jugal. It is a relatively broad element, similar to the postorbital in species of *Phalarodon* (Motani 1999b; Schmitz et al. 2004) and *M. panxianensis* (Jiang et al. 2005, 2006), but different from the slender postorbitals of *M. cornalianus* and *M. kuhnschnyderi* (Brinkmann 2004; Renesto et al. 2020). The jugal forms the ventral and posteroventral margins of the orbit. It is a slender bone, with an approximately straight and narrow anterior ramus and a proportionally broader postorbital ramus. In contrast to the holotype of *M. panxianensis*,

the jugal does not produce a distinct posteroventral process (Jiang et al. 2006).

Some other cranial elements are disarticulated from the rest of the skull and displaced from their original position. The broad quadrate can be seen inside the orbit. It has a large rounded dorsal lamella, and a smaller, stout articular condyle, which bears a transverse groove. The quadrate possesses a small, triangular process, also present in *Besanosaurus* and *Guanlingsaurus* (Bindellini et al. 2021). The basioccipital is exposed in ventral view and is very similar to the basioccipital of *M. cornalianus*, with both possessing an extensive extracondylar area (Maisch et al. 2006; Miedema et al. 2023a). The convex basioccipital condyle is smooth and bears a subtle notochordal pit. The extracondylar area has a midline ridge and protruding lateral wings, with no ventral invagination present (Miedema et al. 2023a). A bone exposed in the lower temporal embayment immediately posterior to the jugal possibly represents the posterolateral part of the pterygoid. The large sheet-like bones visible inside the ventral part of the orbit probably comprise the pterygoids and palatines. Some extremely compressed scleral plates are preserved on the surface of the exposed palatal elements.

Mandible: The two mandibular rami are disarticulated from each other. The left ramus is preserved in anatomical position, but the right ramus underwent a 180° rotation and lies ventral to the skull. As a result, both rami fully expose their medial sides. The Meckelian canal forms a longitudinal groove on the dentary, until it becomes posteromedially closed by the splenial. The splenial produces two long, prong-like processes along the posterodorsal and posteroventral margins of the Meckelian canal, which clearly contact the dentary. However, the sutural contacts between the splenial and the angular and surangular are indeterminate due to numerous surface cracks caused by the collapse of the medial wall of the Meckelian canal. The suture between the dentary and surangular is also indeterminate. The surangular is exposed in the posterodorsal part of the medial wall of the mandibular ramus, and bears a very small paracoronoid process (= coronoid process of Schmitz et al. 2004) (Miedema et al. 2023a). Posteriorly, the prearticular exposes its triangular medial surface. It wedges in between the dorsally positioned surangular and the ventrally positioned angular, and contacts the splenial anteroventrally. The articular comprises the most caudal part of each mandibular ramus. Anteriorly, it bears a shallowly concave articular surface for the quadrate, and possesses a smooth, saddle-shaped medial surface. Two bar-like bones lying between the mandibular rami are interpreted to be the ceratobranchials of the hyoid apparatus. They are straight and have a truncated anterior end.

Dentition: As in most other mixosaurids (with the exception of *P. atavus*; Liu et al. 2013; Engelschiøn et al. 2023), heterodonty is clearly exhibited by HFUT HL-21-08-002. Because the anterior tip of the upper jaw is missing, the most mesial teeth are only preserved in the mandible, whereas middle and distal teeth are well preserved in both the upper jaws and the mandibular rami. The very tip of the lower jaw is edentulous, with the first tooth preserved 6.0 mm posterior to the tip of the left mandibular ramus. This is similar to the condition in *Phalarodon fraasi*, which was also reported to have an edentulous snout tip (Nicholls et al. 1999). The dentary teeth are set in a continuous dental groove, which has a labial wall evidently higher than the lingual wall, and is very pronounced posteriorly. Individual tooth alveoli seem to be absent and some teeth are spaced very closely to each other, so the tooth implantation mode in the dentary can be determined as aulacodonty or subthecodonty (if unexposed sockets are present at the bottom of the dental groove) (Motani 1997b; Bertin et al. 2018). The mode of tooth implantation in the upper jaws in not possible to infer.

The most mesial teeth are extremely small, with the crown height of the first preserved tooth measuring only around 1.1 mm in height and 0.7 mm in basal width (height:width ratio 1.57). More distally, in the middle of the dentigerous region, the teeth become larger and more robust. The posterior dentition bears the largest teeth, with the largest of the fully exposed posterior teeth reaching a crown height of about 2.5 mm and a crown basal width of about 2.1 mm (height:width ratio = 1.19), being more than twice the size of the anterior teeth. The most posterior teeth are smaller than the preceding ones but are more robust, with their crowns being noticeably broadened (mesiodistally), with basal widths exceeding their heights (e.g., the last right dentary tooth has a crown height of 1.7 mm and a crown basal width of 1.8 mm, which gives a height:width ratio of 0.94). There is no shape difference between the corresponding upper and lower teeth.

All teeth, including the posterior ones, have a pointed apex. There are no molariform teeth present, in contrast to *M. kuhnschnyderi*, *M. panxianensis*, *P. callawayi*, and *P. fraasi* (Brinkmann 1998b; Schmitz et al. 2004; Motani 2005a; Jiang et al. 2006; Chen and Cheng 2010). Longitudinal striations can be observed along the entire height of the crown surfaces. The roots have a matte surface texture, different from the shiny crown enamel surface. Many of the roots are mediolaterally flattened, which might reflect the crushing of pulp cavities. No furrows indicating the presence of dentine infolding can be observed in the roots of HFUT HL-21-08-002, which resembles the condition in *M. cornalianus* (Maxwell et al. 2012a), but contrasts with the morphology in other mixosaurids, like species of *Phalarodon* and *M. panxianensis*, in which plicidentine is present (Merriam 1910; Nicholls et al. 1999; Schmitz et al. 2004; Jiang et al. 2006; Chen and Cheng 2010; Maxwell et al. 2012a). In general, the dentition of HFUT HL-21-08-002 is most similar to the dentition of *M. cornalianus* (e.g., PIMUZ T 2418), as both taxa share moderate heterodonty with tiny, mesial-most teeth and stouter, non-molariform posterior teeth (Fig. 4). However, the dentition of both taxa differs in that the distal teeth of *M. cornalianus* are about the same size as the mesial teeth, whereas in HFUT HL-21-08-002 the distal teeth are about twice the size of the mesial teeth.

Fig. 4. A comparison of dentition in species of the mixosaurid ichthyosaur *Mixosaurus*. **A**. *Mixosaurus panxianensis* Jiang et al., 2006, from Panzhou, China, middle Anisian, GMPKU P-1039. **B**. *Mixosaurus kuhnschnyderi* Brinkmann, 1998b, from Monte San Giorgio, Italy and Switzerland, upper Anisian–lower Ladinian, PIMUZ T 1324. **C**. *Mixosaurus cornalianus* (Bassani, 1886) from Monte San Giorgio, Italy and Switzerland, upper Anisian–lower Ladinian, PIMUZ T 2418. **D**. *Mixosaurus luxiensis* sp. nov. from Luxi, China, middle Anisian, HFUT HL-21-08-002. B and C depict the mandibular dentition only. Scale bars 10 mm.

Axial skeleton: The majority of the vertebral column is disarticulated, but three cervical neural arches (2–4) and the middle caudal vertebrae are preserved as articulated series. Only the axial neural arch is articulated with its corresponding centrum (axis), whereas the two other neural arches are isolated. The neural spine of the axis is trapezoid in outline and bears a vertical groove on its lateral surface. It is 10 mm high and 8 mm wide at its base and is markedly broader than the subsequent cervical neural spines. All three preserved cervical neural arches bear suboval, dorsoventrally elongated diapophyses, which articulated with the tuberculum of the bicipital cervical ribs (SOM 1: fig. S1). This condition is similar to the one reported for *Phalarodon callawayi*, in which the diapophysis is also located on the cervical neural arch (Schmitz et al. 2004). Anteriorly projecting prezygapophyses and posteriorly projecting postzygapohyses are well-developed in the cevical neural arches.

The amphicoelous posterior dorsal and anterior caudal centra are disarticulated and scattered in the posterior portion of the specimen and their corresponding neural arches are also disarticulated and often broken. Several hexagonal (in articular view) and mediolaterally compressed centra, representing the more posterior caudal centra, are also scattered in the same area. Most dorsal centra possess single rib facets, but some centra located close to the sacral region have double rib facets. In the middle dorsal region, the centra vary from about 8–9 mm in height and 6–7 mm in length, with their corresponding neural arches reaching up to 20 mm in height. In the posterior dorsal/anterior caudal region, centra achieve their maximum size, the largest being over 10 mm in height and around 7–8 mm in length. The longest neural spine from this region is about 21 mm tall.

A series of 18 consecutive centra and two incomplete neural spines, measuring 112.9 mm in total length, comprises the most posterior part of the preserved vertebral column (SOM 1: fig. S2, table S2). Based on the relative length and orientation of the neural spines, as well as the disappearance of rib facets in the seventh centrum in the preserved series, these vertebrae can be confidently identified as representing the caudal peak and its immediate vicinity. The centrum height/length ratios in the centra located immediately posterior to the caudal peak are only

around 2.0, which is also characteristic for *M. cornalianus* (Nicholls et al. 1999; Schmitz et al. 2004; Schmitz 2005). On the dorsal side of the articulated caudal series, most of the neural spines located posterior to the caudal peak are clearly visible. In the posterior part of the articulated caudal series, the slender haemal arches (chevrons) articulate between the adjacent centra.

The ribs in the anterior trunk region are largely fractured and fragmented. The posterior ribs are more completely preserved, the longest measuring up to 100 mm in chord length. The dorsal ribs of HFUT HL-21-08-002 possess a single head, are slightly expanded at their distal ends, and possess a longitudinal furrow on their anterior/posterior surfaces. Clusters of slender, disarticulated gastral elements are preserved in the ventral part of the specimen. Several boomerang-shaped median gastral elements can be recognised, some of them bearing a short anterior process. The lateral gastral elements are needle-like and mostly straight.

Appendicular skeleton: The elements of the pectoral girdle and forelimbs are partly disarticulated and expose their flattened surfaces (Fig. 5). The left forefin and the left coracoid are partially overlapped by their right counterparts, whereas the outline of the glenoid process of the left coracoid is embossed on the right coracoid. The right coracoid measures 47 mm in length, whereas the width of the left coracoid equals 27.3 mm. The right scapula is of similar size to the coracoids, measuring 46 mm in length and 27.5 mm in width. The coracoids and scapula are fan-shaped, like in other mixosaurids and other basal ichthyopterygians (McGowan and Motani 2003). The scapula is approximately symmetrical, whereas the glenoid processes of the coracoids are situated much more posteriorly, making the coracoids asymmetric. The interclavicle is preserved in dorsal view, attached to the anteromedial margin of the left coracoid. Its anterior edge bears articular facets for the clavicles. The triradiate interclavicle possesses broad transversal bars and a relatively shorter posterior process. The general shape of the interclavicle resembles the interclavicles of *M. kuhnschnyderi*, *M.* cf. *cornalianus* Type A, and some Chinese mixosaurids (e.g., CCCGS LPV 30986, GMPKU P-1065; Liu 2011; Zang 2014) more than the interclavicle of *M. cornalianus* Type B (posterior process longer than the transversal bars, e.g. PIMUZ T 2420 [neotype]) (Brinkmann 1998a, 1999, 2004; Jiang et al. 2006). The clavicles are slender, gently curved, rod-like bones, partly covered by the right scapula and right coracoid. The outlines of the clavicles are also partly embossed on the coracoids. The left clavicle is preserved in articulation with the interclavicle, whereas the contralateral clavicle is disarticulated and displaced anteriorly.

The right forelimb of HFUT HL-21-08-002 is exposed from its dorsal side. The length of the humerus is 24.1 mm, and its maximum width at the distal end is 19.6 mm. Compared with the relatively more elongated humerus in species of *Phalarodon* (Motani 1999a; Brinkmann 2004; Schmitz et al. 2004; Jiang et al. 2006; Liu 2011), it is more similar to the humeri in other species of *Mixosaurus* (Maisch and Matzke 1998b; Kolb et al. 2011; Zhou et al. 2022). The radius is 19.9 mm long, 11.4 mm wide proximally and 12.5 mm wide distally. The slenderness of the radius (proximodistal length/midshaft width ratio = 2.4) differs from other *Mixosaurus* species, in which the length/width ratio of the radius <2 (Brinkmann 2004; Zhou et al. 2022). Anteriorly, the leading (anterior) edge of the radius bears two shallow notches located proximally and distally, with the middle portion situated between the notches forming a convex margin. The maximum mid-length width of the radial shaft is 8.4 mm, whereas its narrowest width at the notches is 7.6 mm. The two notches on the leading edge of the radius were regarded as a unique feature of *M. panxinensis* (Jiang et al. 2006; Maisch 2010), but they also occur in *Mixosaurus* from the Luoping Biota (e.g., CCCGS LPV 30986, YIGMR SPCV-0810, and YIGMR SPCV-0831, Chen and Cheng 2009; Liu 2011; Chen et al. 2016) and several specimens of European *Mixosaurus* (e.g., SMNS 54068, Zhou et al. 2022; the fetus of PIMUZ T 2262, Miedema et al. 2023b). The approximately lunate ulna bears a prominent notch on its trailing (posterior) edge. The posterior notch of the ulna is rare among mixosaurids, but was reported in referred specimens of *M. panxianensis* (GMPKU P-1038, GMPKU P-1065, Zang 2014; Zhou et al. 2022), "*M. xindianensis*" (YIGMR SPCV-0732, Chen and Cheng 2010) and *Phalarodon callawayi* (PMU 45386 [= PMU R 191 in Motani 1999a; Schmitz et al. 2004]). The ulna has a proximodistal length of 18.3 mm, a proximal width of 11.4 mm, a distal width of 13.0 mm and its narrowest width at the notch equals 8.3 mm.

The proximal portion of the right manus is disarticulated to some extent, whereas the distal parts of both the left and right manus are preserved in articulation. The right manus is completely preserved, but some of its elements are covered by disarticulated gastralia and its trailing edge is largely obscured by gastralia and ribs. Four proximal carpals including a round pisiform can be discerned, and the distal carpals are preserved in close association with the corresponding proximal carpals. The pisiform is partly obscured by the ulna. The pentagonal intermedium comprises the largest carpal. It is wider than long, having a width of 9.6 mm and a length of 8.0 mm. The distal carpals are smaller than the proximal carpals. Distal carpals I, III, IV are quadrangular in outline, whereas distal carpal II is pentagonal. The metacarpals and proximal phalanges are hourglass-shaped and are similar to each other, except for metacarpals I and V. These two metacarpals are broader, metacarpal I being subquadrangular in outline, and the dislocated metacarpal V being suboval and probably bearing a notch. HFUT HL-21-08-002 shares the presence of a large (much larger than distal carpal IV) and notched metacarpal V with some mixosaurids from Luoping (e.g., CCCGS LPV 30872, 30986, Liu 2011; Liu et al. 2013). However, whereas the notch is located anterodistally in metacarpal V of mixosaurids from Luoping, metacarpal V in HFUT HL-21-08-002 is disarticulated and the

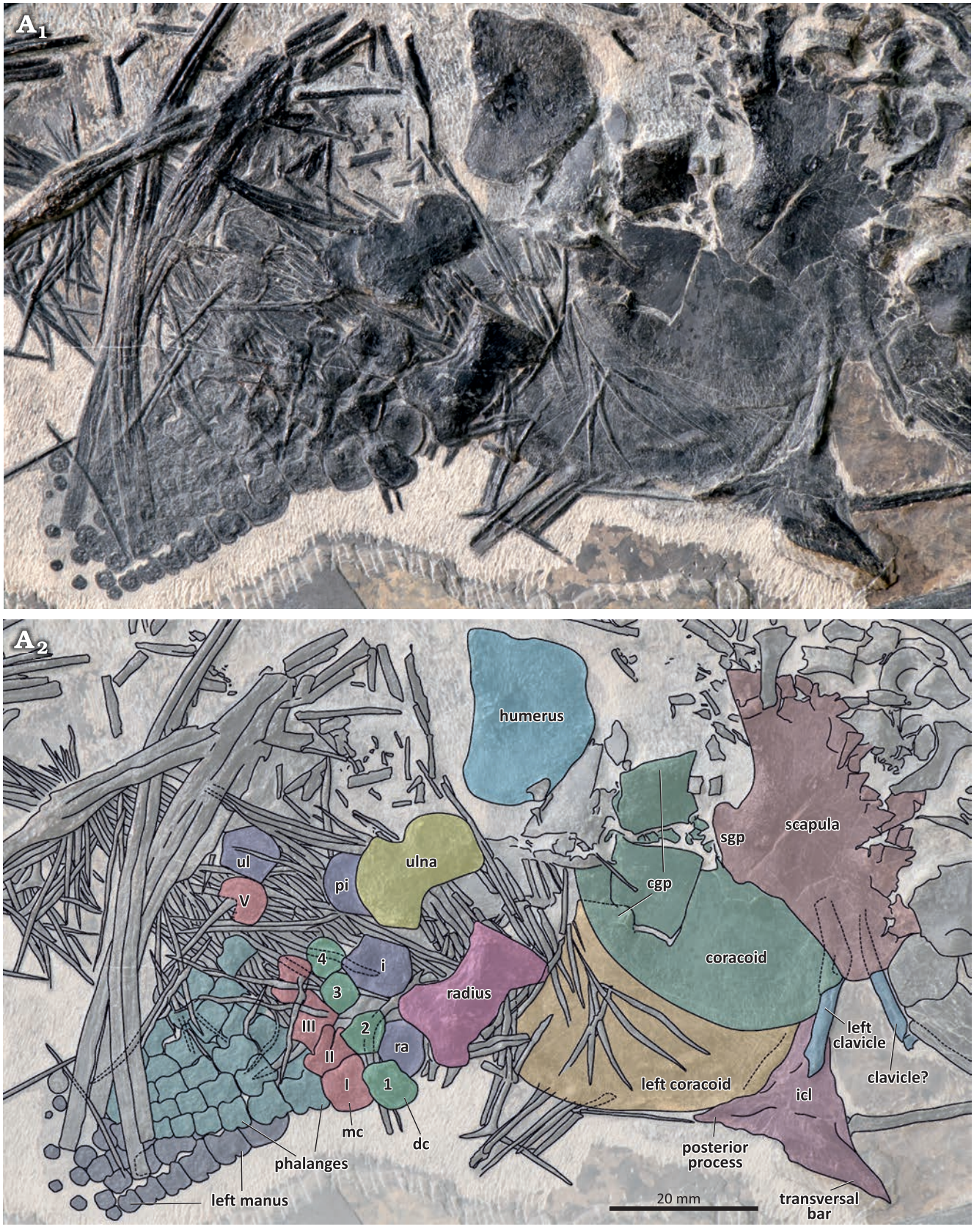

Fig. 5. The pectoral girdle and forefins of the mixosaurid ichthyosaur *Mixosaurus luxienis* sp. nov. (HFUT HL-21-08-002) from Huale Village, Luxi County, Yunnan Province, China (Pelsonian, Anisian). Photograph (A_1) and interpretative drawing (A_2). Dashed lines indicate inferred margins. Abbreviations: cgp, glenoid process of coracoid; dc 1–4, distal carpals 1–4; i, intermedium; icl, interclavicle; mc I–V, metacarpals I–V; pi, pisiform; ra, radiale; sgp, glenoid process of scapula; ul, ulnare.

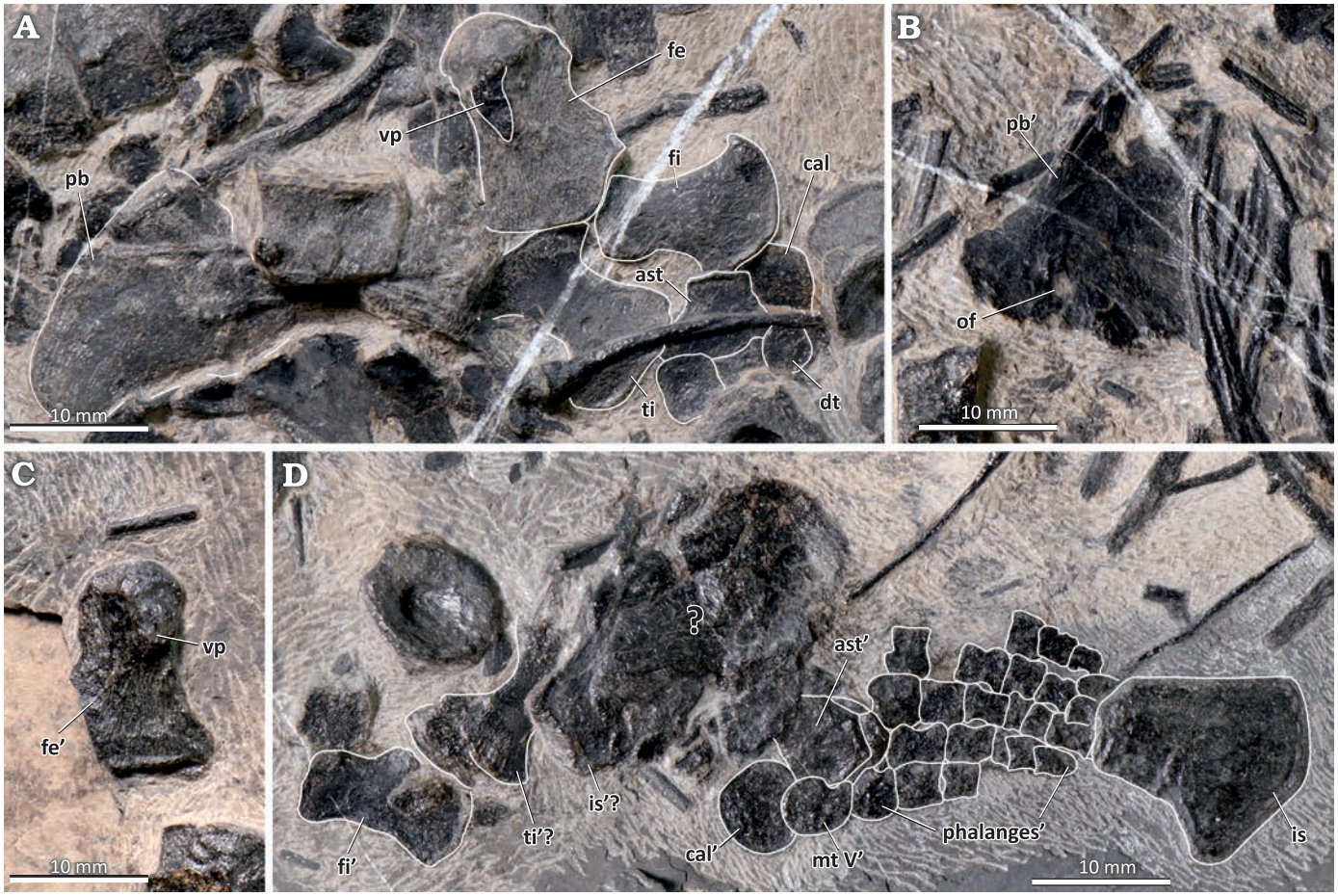

Fig. 6. The pelvic girdle and hindfins of the mixosaurid ichthyosaur *Mixosaurus luxiensis* sp. nov. (HFUT HL-21-08-002) from Huale Village, Luxi County, Yunnan Province, China (Pelsonian, Anisian). **A**. Right pubis and right hindlimb elements. **B**. Left pubis. **C**. Left femur in ventral view. **D**. Left ischium and left hindlimb. Dashed lines indicate inferred margins; the ' symbol indicates left elements. Abbreviations: ast, astragalus; cal, calcaneum; dt, distal tarsal; fe, femur; fi, fibula; is, ischium; mt, metatarsal; of, obturator foramen; pb, pubis; ti, tibia; vp, ventral process of femur.

element could have undergone rotation, so it is not possible to determine its exact orientation in the latter. The elements in digit I are shorter than the corresponding elements in digit II, which is clearly visible in the third phalangeal row. All phalanges (except the most distal ones) in digit I have a notched leading edge, a feature that is also typical for *M. panxianensis* but absent in *M. cornalianus* (Maisch and Matzke 1998b; Motani 1999a; Renesto et al. 2020; Zhou et al. 2022). The most distal phalanges do not possess a mid-shaft constriction and appear rounded in shape. The distal part of the left forelimb is partially visible ventral to the right forelimb and exposed in ventral view. Its phalangeal morphology is consistent with that of its right counterpart.

The bones comprising the pelvic girdle and hindlimbs are scattered in the posterior part of the specimen (Fig. 6). The plate-like pubes are partially preserved and exposed in ventral or dorsal view. One pubis is located near the right hindlimb and is relatively complete, whereas the other lies near the ribcage, is partially damaged, and encloses an obturator foramen. A single identifiable ischium is fan-shaped and is located in the ventral part of the fossil. Both femora are exposed in ventral view with the prominent ventral process clearly visible, extending from the femoral head to the mid-shaft region (Maxwell et al. 2012b). The expanded distal end is wider than the rounded proximal head and has clearly demarcated tibial and fibular facets. The right femur (length 16.6 mm, distal width 11.5 mm) lies closely to the more completely preserved pubis and is loosely connected with the zeugopodium, whereas the left femur is disarticulated and dislocated from the remainder of the left hindlimb. The length of the right tibia equals 13.5 mm, and the widths of its expanded proximal and distal ends are 9.4 mm and 9.9 mm, respectively. The distal end of the fibula (length 13.2 mm) is distinctly expanded. The left zeugopodium, which is similar in shape and size to its right counterpart, is located near a cluster of indeterminate, flattened bones. These bones probably represent some of the other elements of the pelvic region but cannot be identified with confidence.

The right tarsals are loosely connected to the zeugopodium—the astragalus, calcaneum and three distal tarsals can be discerned. The more distal metatarsals and phalanges of the right hindlimb are partly concealed by the scattered ribs and centra, but these elements are well-preserved in the left autopodium. Among the left tarsals, the sub-

circular calcaneum and polygonal astragalus are the most conspicuous. Metatarsal V is oval in outline and has a small anterior notch. Distally, the metatarsals and phalanges in the left hindfin are heavily abraded and extremely compressed, so that the individual elements are very difficult to discern. The elements in digits III and IV are longer than the corresponding elements in digit V.

Stratigraphic and geographic range.—Type locality and horizon only.

Discussion

Several morphological character states distinguish *Mixosaurus luxiensis* sp. nov. from other species of *Mixosaurus*. The wider post-orbital region distinguishes it from *M. cornalianus* and *M. kuhnschnyderi* from the Grenzbitumenzone/Besano Formation (Brinkmann 1998a, 2004; Renesto et al. 2020). Additionally, the sagittal crest of *M. luxiensis* sp. nov. does not extend anteriorly as much as in other mixosaurids, and contrasts especially with *M. panxianensis*, the sagittal crest of which extends anteriorly beyond the external naris (Jiang et al. 2005, 2006).

Heterodonty in Mixosauridae is present in the majority of its members, with only *Mixosaurus* cf. *cornalianus* Type A and *Phalarodon atavus* being the exceptions and exhibiting isodonty (Brinkmann 1998a, 2004; Liu et al. 2013). The distal teeth differ interspecifically among mixosaurids, from being simple and stout (e.g., *M. cornalianus*, Bassani 1886; Brinkmann 1998a, 2004) to being markedly molariform, flattened and mediolaterally compressed (e.g., *P. fraasi*, Nicholls et al. 1999; Motani 2005a; Økland et al. 2018; Roberts et al. 2022), and are diagnostic at the species level (Brinkmann 1998a, 2004; Motani 1999b; McGowan and Motani 2003). The dentition of *M. luxiensis* sp. nov. can be easily differentiated from that of *M. panxianensis*, with the latter having conspicuous molariform teeth (especially in the posterior part of the mandible) and infolded dentine (Jiang et al. 2006). The dentition of *M. luxiensis* sp. nov. also contrasts with the dentition of *M. kuhnschnyderi*, which has mesiodistally elongated posterior dentary teeth without a pointed apex (Brinkmann 1998a, b, 2004). In general, *M. cornalianus* resembles *M. luxiensis* sp. nov. the most in its dentition. The difference is that the posterior teeth of *M. luxiensis* sp. nov. are more than twice the size of the anterior teeth, whereas the posterior teeth remain very small in *M. cornalianus* (Repossi 1902; Miedema et al. 2023a).

Zhou et al. (2022) provided a comprehensive description of forefin variability in *M. panxianensis* spanning a range of body sizes. The two notches on the leading edge of the radius were shown to be present in all specimens representing different growth stages. *M. cornalianus* and *M. kuhnschnyderi* were thought to have a complete peripheral shaft on the radius (Maisch and Matzke 1998b, Brinkmann 2004; also see the character scores in the matrices of Ji et al. 2016, Motani et al. 2017 and Huang et al. 2019), but similar double notches can also be observed in some other *M. cornalianus* specimens (e.g., SMNS 54068, Zhou et al. 2022). Despite sharing the presence of two notches on the leading edge of the radius with *M. panxianensis* and *M. cornalianus*, the radius of *M. luxiensis* sp. nov. differs not only from *M. panxianensis*, but also from all other species of *Mixosaurus*, in its slenderness. The ratio of radius proximodistal length to midshaft width at flange in *M. luxiensis* sp. nov. is 2.4 (19.9 mm/8.2 mm), in comparison with a ratio of 1.5–1.9 in *M. panxianensis* (sample size = 6, Xiong 2020; Zhou et al. 2022) and *M. cornalianus* (sample size = 20, Maisch and Matzke 1998b; Motani 1999a; Renesto et al. 2020; Zhou et al. 2022; JL personal observation of SMNS and PIMUZ specimens). *M. kuhnschnyderi* also has a slender radius, but the length/width ratio (1.9) in PIMUZ T 1324 is still lower than that in *M. luxiensis* sp. nov. and more comparable with those in *M. panxianensis* or *M. cornalianus*. The ulnar peripheral notch and notching on the leading edge of proximal phalanges in digit I are absent in *M. cornalianus*, although mid-digit notching on the leading edge of digit I was reported in large specimens (Maxwell et al. 2014). Another feature in which *M. luxiensis* sp. nov. is distinct from *M. panxianensis* and *M. cornalianus* is the relatively large size of metacarpal V compared with the adjacent distal carpal IV. However, it is worth noting that Liu et al. (2013) regarded this feature as diagnostic for *Phalarodon atavus* (CCCGS LPV 30872) collected from Luoping. In addition, other mixosaurids recovered from Luoping also possess a proportionally large metacarpal V (e.g., CCCGS LPV 30281, 30986, 31880, Liu 2011; JL personal observation]), so this feature is probably more widespread in mixosaurids than previously thought, particularly in those species from the Luoping and Luxi faunas. This is interesting, because this feature is absent in mixosaurids from the Panxian fauna, which is similar in age (Pelsonian, Anisian) and located nearby geographically. The proportionally narrow radius, the unique shape and large size of metacarpal V, the notch on the posterior margin of the ulna, and the relatively elongated phalanges in digit II of *M. luxiensis* sp. nov. are also reminiscent of the ancestral conditions present in basal ichthyopterygians (e.g., *Grippia*, *Utatsusaurus*) (Motani 1997a, 1998, 1999a). This may indicate that these features represent ichthyopterygian plesiomorphies retained in *M. luxiensis* sp. nov. but lost in some other mixosaurids (e.g., *M. cornalianus*) (Liu et al. 2013).

The genus *Phalarodon* can be confidently distinguished from *M. luxiensis* sp. nov. by a series of autapomorphies, such as the V-shaped interclavicle, relatively narrow humerus and relatively high centrum height/length ratio (Motani 1999a; Nicholls et al. 1999; Schmitz et al. 2004; Schmitz 2005; Jiang et al. 2006; Økland et al. 2018). *Phalarodon atavus* (LPV 30872) from the Luoping fauna has a unique radius morphology with an extremely constricted shaft, but also shares some similarities with *M. luxiensis* sp. nov. in forefin morphology (e.g., a large, notched metacarpal V) and caudal centrum height index (maximum height/length ratio around

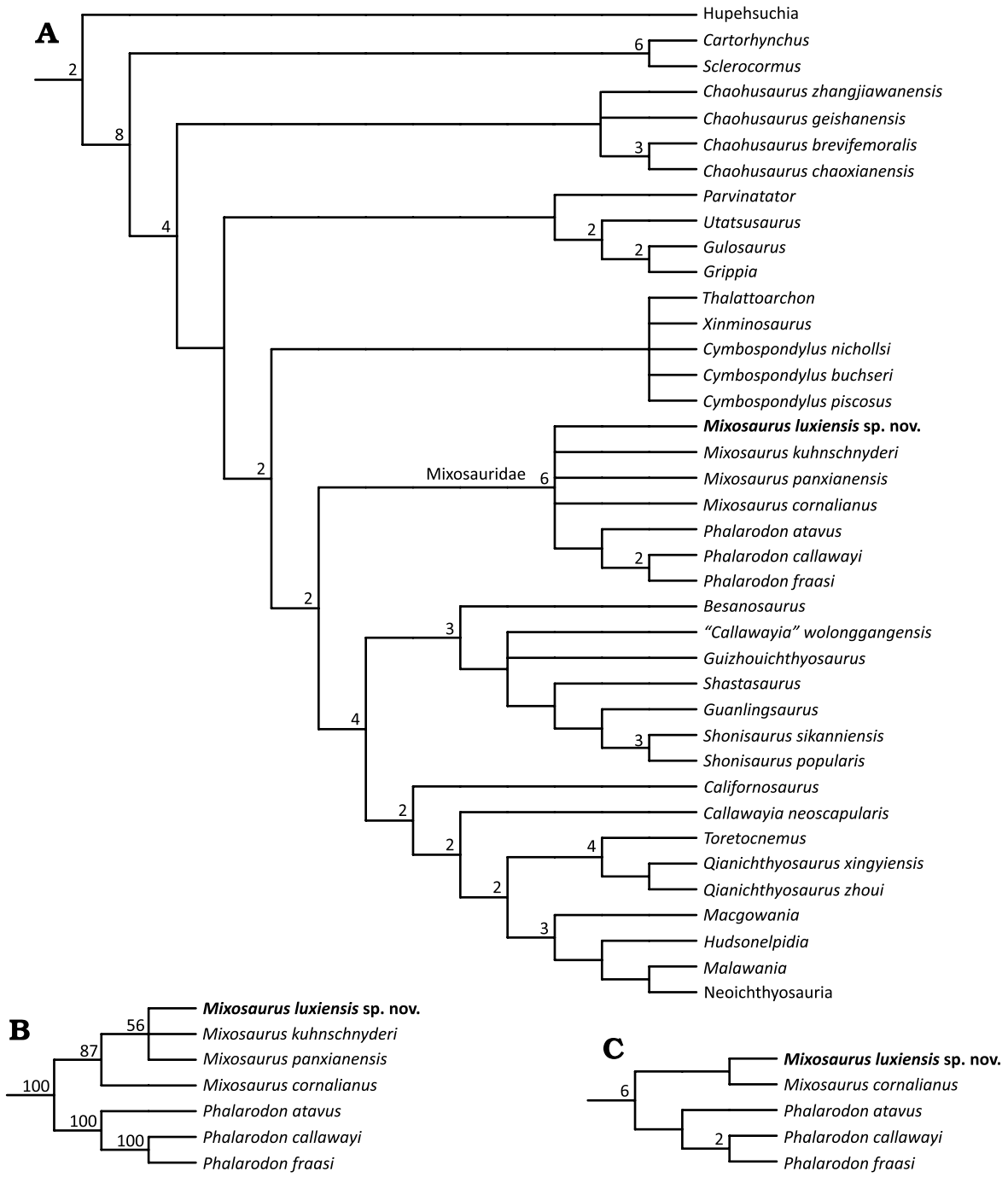

Fig. 7. The phylogenetic position of *Mixosaurus luxiensis* sp. nov. within Ichthyosauromorpha. **A**. Strict consensus tree, with Bremer values larger than 1 indicated at relevant nodes. **B**. The topology of Mixosauridae obtained in the 50% majority rule consensus tree, with the percentages of MPTs in which a particular clade is recovered given at relevant nodes. **C**. The reduced strict consensus tree of Mixosauridae obtained through IterPCR, with Bremer values larger than 1 indicated at relevant nodes. See Material and methods for analytical procedure.

2.0) (Liu et al. 2013). On the other hand, Muschelkalk specimens of the same taxon differ from *M. luxiensis* sp. nov. in possessing a sagittal crest extending anteriorly beyond the external naris, a larger parietal, and widely spaced distal teeth (Maisch and Matzke 2001). GMPKU P-1032 is the only reliably identified specimen of *Phalarodon* from the Panxian fauna (Jiang et al. 2007). The presence of a narial shelf and the mesiodistally elongated molariform teeth differentiate it from *M. luxiensis* sp. nov.

The Middle Triassic strata of South China have yielded abundant fossils of mixosaurids over the past decades, but their taxonomic diversity is incompletely understood. All of the previously erected *Mixosaurus* species have distinctive morphological features that differentiate it from *M. luxiensis* sp. nov. The differences between *M. luxiensis* sp. nov. and *M. panxianensis* have already been discussed. The earliest mixosaurid reported from South China, "*M. maotaiensis*", lacks valid diagnostic character states and is considered a

nomen dubium (Young 1965; McGowan and Motani 2003; Jiang et al. 2006). "*M. yangjuanensis*" was erected for some mixosaur specimens from the Panxian Fauna, but is similar to *M. panxianensis* in its dentition and forefin morphology (Jiang et al. 2008a; Liu and Yin 2008). A referred specimen of "*M. cornalianus*" reported by Liu and Yin (2008) was likely also incorrectly identified (Jiang et al. 2008a). Chen and Cheng (2009) reported a small mixosaurid from the Luoping fauna (YIGMR SPCV-0810) that they referred to *M. kuhnschnyderi*. It differs from *M. luxiensis* sp. nov. in the presence of a narrow postorbital, absence of the ulnar notch and the presence of molariform teeth.

"*M. xiandianensis*" was erected based on a single, largely complete specimen (YIGMR SPCV-0732) from the Panxian Fauna (Chen and Cheng 2010). Its deep lower temporal embayment resembles that of *M. panxianensis*, but the presence of single peripheral notches on the radius and ulna differentiate it from *M. panxianensis*. Furthermore, the presence of the narial shelf and the buccal ridge and the high centrum height/length ratio (up to 3.3 in the caudal region) of YIGMR SPCV-0732 imply a *Phalarodon* affinity of the specimen (Chen and Cheng 2010). In addition to the features mentioned above, "*M. xiandianensis*" differs from *M. luxiensis* sp. nov. by the presence of durophagous dentition and the lack of the dental groove. Chen et al. (2016) named "*M. xinzhaiensis*" based on a single, mostly complete specimen (YIGMR SPCV-0831) from the Luoping fauna. "*M. xinzhaiensis*" differs from *M. luxiensis* sp. nov. in that its postorbital participates in the margin of the upper temporal fenestra and the prefrontal participates in the margin of the external naris.

The phylogenetic analysis recovered 90 most parsimonious trees (MPTs) with a length of 715 steps (CI = 0.362, RI = 0.789). In the strict consensus tree, Mixosauridae form a polytomy, with only *Phalarodon* recovered as a monophyletic clade. In the 50% majority rule consensus tree, the monophyly of *Mixosaurus* is recovered in 87% of MPTs. To provide better resolution for the Mixosauridae node, we used IterPCR to identify and prune the unstable taxa *M. panxianensis* and *M. kuhnschnyderi*. The resulting reduced consensus tree further supports the clade comprising *M. cornalianus* and *M. luxiensis* sp. nov., to the exclusion of all *Phalarodon* species (Fig. 7). It is not surprising that eastern and western Tethyan mixosaurid taxa could be closely related, as demonstrated for fish and other marine reptile taxa (Jiang et al. 2008b; Liu et al. 2013; Tintori et al. 2017). However, it must be pointed out that the only unambiguous synapomorphies that unite *M. luxiensis* sp. nov. with *M. cornalianus* are the relatively small tooth size and the lack of dentary labial shelf. Furthermore, since not all of the species of mixosaurids from South China currently recognised as valid are included in the phylogenetic analysis presented here and some of the important anatomical features differentiating various mixosaurids are not incorporated as characters in the phylogenetic matrix, the cladistic topology obtained in this study should be treated as preliminary. Therefore, further studies of mixosaurid anatomy and the incorporation of their morphological variation into existing phylogenetic matrices for ichthyosaurs are needed to understand the phylogeny of mixosaurids in more detail. This, in turn, will provide us with a better understanding of their evolution and history of geographical dispersal between Europe, North America and South China.

Conclusions

A mixosaur specimen from Luxi County, Yunnan Province is described in detail. HFUT HL-21-08-002 represents a new taxon, *Mixosaurus luxiensis* sp. nov., distinguished from other species of *Mixosaurus* by a unique combination of cranial, dental and postcranial character states. The dentition of *M. luxiensis* sp. nov. resembles the dentition of *M. cornalianus* from Europe the most, but its forelimb shares more similarities with mixosaurids from the Luoping Biota in South China. The preliminary phylogenetic analysis recovers *M. luxiensis* sp. nov. as the sister taxon of *M. cornalianus*. Our study highlights the morphological diversity of *Mixosaurus* from South China and emphasises the necessity of further studies on the anatomy and evolutionary history of mixosaurids.

Acknowledgements

We thank Liang-You Li (HFUT) for the preparation of the specimen, members of the Hefei University of Technology Vertebrate Paleontology Research Group for participation in field work and Li-Yan Men (HFUT) for help with photography. We also thank Yi-Wei Hu (HFUT) for providing the original version of the geological map of the Luxi area. We thank the following curators for providing us access to specimens under their care: Long Cheng (WCCGS), Da-Yong Jiang and Min Zhou (both GMPKU), Benjamin Kear (PMU), Erin Maxwell (SMNS), and Christian Klug and Torsten Scheyer (both PIMUZ). We thank Daniel E. Barta (Oklahoma State University, Tahlequah, USA), E. Maxwell, and another anonymous reviewer for constructive suggestions, and the The Willi Hennig Society for making TNT 1.5 freely available. The work was supported by the National Natural Science Foundation of China (grant numbers 42172026, 41772003, and 42202006), the Chinese Postdoctoral Science Foundation, and Bekker Programme of the Polish National Agency for Academic Exchange (grant number BPN/BEK/2022/1/00194).

References

Bambach, R.K. 2006. Phanerozoic biodiversity mass extinctions. *Annual Review of Earth and Planetary Sciences* 34: 127–155.

Bardet, N., Falconnet, J., Fischer, V., Houssaye, A., Jouve, S., Pereda Suberbiola, X., Pérez-García, A., Rage, J.-C., and Vincent, P. 2014. Mesozoic marine reptile palaeobiogeography in response to drifting plates. *Gondwana Research* 26: 869–887.

Bassani, F. 1886. Sui fossili e sull'età degli schisti bituminosi Triasici di Besano in Lombardia. Communicazione preliminare. *Atti della Società Italiana di Scienze Naturale* 29: 15–72.

Baur, G. 1887. On the morphology and origin of the Ichthyopterygia. *American Naturalist* 21: 837–840.

Benton, M.J., Zhang, Q.-Y., Hu, S.-X., Chen, Z.-Q., Wen, W., Liu, J., Huang, J.-Y., Zhou, C.-Y., Xie, T., Tong, J.-N., and Choo, B. 2013. Exceptional vertebrate biotas from the Triassic of China, and the expansion of marine ecosystems after the Permo-Triassic mass extinction. *Earth-Science Reviews* 125: 199–243.

Bertin, T.J.C., Thivichon-Prince, B., LeBlanc, A.R.H., Caldwell, M.W., and Viriot, L. 2018. Current perspectives on tooth implantation, attachment, and replacement in amniota. *Frontiers in Physiology* 9: 1630.

Bindellini, G., Wolniewicz, A.S., Miedema, F., Scheyer, T.M., and Dal Sasso, C. 2021. Cranial anatomy of *Besanosaurus leptorhynchus* Dal Sasso & Pinna, 1996 (Reptilia: Ichthyosauria) from the Middle Triassic Besano Formation of Monte San Giorgio, Italy/Switzerland: taxonomic and palaeobiological implications. *PeerJ* 9: e11179.

Blainville, H.M.D. 1835. Description de quelques espèces de reptiles de la Californie: précédée de l'analyse d'un systéme général d'erpétologie et d'amphibiologie. *Nouvelles Annales du Muséum d'Histoire Naturelle* 4: 233–296.

Brayard, A., Krumenacker, L.J., Botting, J.P., Jenks, J.F., Bylund, K.G., Fara, E., Vennin, E., Olivier, N., Goudemand, N., Saucède, T., Charbonnier, S., Romano, C., Doguzhaeva, L., Thuy, B., Hautmann, M., Stephen, D.A., Thomazo, C., and Escarguel, G. 2017. Unexpected Early Triassic marine ecosystem and the rise of the Modern evolutionary fauna. *Science Advances* 3 (2): e1602159.

Brinkmann, W. 1996. Ein Mixosaurier (Reptilia, Ichthyosauria) mit Embryonen aus der Grenzbitumenzone (Mitteltrias) des Monte San Giorgio (Schweiz, Kanton Tessin). *Eclogae Geologicae Helvetiae* 89: 1321–1344.

Brinkmann, W. 1997. Die Ichthyosaurier (Reptilia) aus der Mitteltrias des Monte San Giorgio (Tessin, Schweiz) und von Besano (Lombardei, Italien) – der aktuelle Forschungsstand. *Vierteljahrsschrift der Naturforschenden Gesellschaft in Zurich* 142 (2): 69–78.

Brinkmann, W. 1998a. Die Ichthyosaurier (Reptilia) aus der Grenzbitumenzone (Mitteltrias) des Monte San Giorgio (Tessin, Schweiz) – neue Ergebnisse. *Vierteljahresschrift der naturforschenden Gesellschaft in Zürich* 143 (4): 165–177.

Brinkmann, W. 1998b. *Sangiorgiosaurus* n. g. – eine neue Mixosaurier Gattung (Mixosauridae, lchthyosauria) mit Quetschzähnen aus der Grenzbitumenzone (Mitteltrias) des Monte San Giorgio (Schweiz, Kanton Tessin). *Neues Jahrbuch für Geologie und Paläontologie, Abhandlungen* 207: 125–144.

Brinkmann, W. 1999. *Ichthyosaurus cornalianus* Bassani, 1886 (currently *Mixosaurus cornalianus*; Reptilia, Ichthyosauria): proposed designation of a neotype. *The Bulletin of Zoological Nomenclature* 56: 247–249.

Brinkmann, W. 2004. Mixosaurier (Reptilia, Ichthyosauria) mit Quetschzähnen aus der Grenzbitumenzone (Mitteltrias) des Monte San Giorgio (Schweiz, Kanton Tessin). *Schweizerische Paläontologische Abhandlungen* 124: 1–84.

Callaway, J.M. 1989. *Systematics, Phylogeny, and Ancestry of Triassic Ichthyosaurs*. xiii + 204 pp. University of Rochester, New York.

Callaway, J.M. 1997. A new look at *Mixosaurus*. *In*: J.M. Callaway and E.L. Nicholls (eds.), *Ancient Marine Reptiles*, 45–59. Academic Press, San Diego.

Callaway, J.M. and Brinkman, D.B. 1989. Ichthyosaurs (Reptilia, Ichthyosauria) from the Lower and Middle Triassic Sulphur Mountain Formation, Wapiti Lake area, British Columbia, Canada. *Canadian Journal of Earth Sciences* 26: 1491–1500.

Carroll, R.L. 1997. Mesozoic marine reptiles as models of long-term, large-scale evolutionary phenomena. *In*: J.M. Callaway and E.L. Nicholls (eds.), *Ancient Marine Reptiles*, 467–489. Academic Press, San Diego.

Chen, X.-H. and Cheng, L. 2009. The discovery of *Mixosaurus* (Reptilia: Ichthyopterygia) from the Middle Triassic of Luoping, Yunnan Province [in Chinese, with English abstract]. *Acta Geologica Sinica* 83: 1214–1220.

Chen, X.-H. and Cheng, L. 2010. A new species of *Mixosaurus* (Reptilia: Ichthyosauria) from the Middle Triassic of Pu'an, Guizhou, China [in Chinese, with English abstract]. *Acta Palaeontologica Sinica* 49: 251–260.

Chen, X.-H., Cheng, L., Wang, C.-S., and Zhang, B.-M. 2016. Chapter 5 Ichthyosaurs [in Chinese]. *In*: X.-L. Qi, X.-R. Yu, and Y. Tian (eds.), *Triassic Marine Reptile Faunas from Middle and Upper Yangtze Areas and Their Co-Evolution with Environment* [in Chinese], 101–161. Geological Publishing House, Beijing.

Chen, Z.Q. and Benton, M.J. 2012. The timing and pattern of biotic recovery following the end-Permian mass extinction. *Nature Geoscience* 5 (6): 375–383.

Dai, X., Davies, J.H.F.L., Yuan, Z., Brayard, A., Ovtcharova, M., Xu, G.-H., Liu, X., Smith, C.P.A., Schweitzer, C.E., Li, M.-T., Perrot, M.G., Jiang, S.-Y., Miao, L.-Y., Cao, Y.-R., Yan, J., Bai, R.-Y., Wang, F.-Y., Guo, W., Song, H., Tian, L., Dal Corso, J., Liu, Y.-T., Chu, D.-L., and Song, H.-J. 2023. A Mesozoic fossil lagerstätte from 250.8 million years ago shows a modern-type marine ecosystem. *Science* 379: 567–572.

Engelschiøn, V.S., Roberts, A.J., With, R., and Hammer, Ø. 2023. Exceptional X-Ray contrast: Radiography imaging of a Middle Triassic mixosaurid from Svalbard. *PLoS ONE* 18 (5): e0285939.

Friesenbichler, E., Hautmann, M., and Bucher, H. 2021. The main stage of recovery after the end-Permian mass extinction: taxonomic rediversification and ecologic reorganization of marine level-bottom communities during the Middle Triassic. *PeerJ* 9: e11654.

Fröbisch, N.B., Fröbisch, J., Sander, P.M., Schmitz, L., and Rieppel, O. 2013. Macropredatory ichthyosaur from the Middle Triassic and the origin of modern trophic networks. *Proceedings of the National Academy of Sciences* 110: 1393–1397.

Goloboff, P.A. and Catalano, S.A. 2016. TNT version 1.5, including a full implementation of phylogenetic morphometrics. *Cladistics* 32: 221–238.

Hu, S.-X., Zhang, Q.-Y., Chen, Z.-Q., Zhou, C.-Y., Lü, T., Xie, T., Wen, W., Huang, J.-Y., and Benton, M.J. 2011. The Luoping biota: exceptional preservation, and new evidence on the Triassic recovery from end-Permian mass extinction. *Proceedings of the Royal Society B: Biological Sciences* 278: 2274–2282.

Hu, Y.-W. and Liu, J. 2023. A new morphotype of nothosaurs (Sauropterygia: Nothosauridae) from the Middle Triassic of South China. *Historical Biology* 35: 1794–1803.

Hu, Y.-W., Li, Q., and Liu, J. 2024. A new pachypleurosaur (Reptilia: Sauropterygia) from the Middle Triassic of southwestern China and its phylogenetic and biogeographic implications. *Swiss Journal of Palaeontology* 143: 1–15.

Huang, J.-D., Motani, R., Jiang, D.-Y., Tintori, A., Rieppel, O., Zhou, M., Ren, X.-X., and Zhang, R. 2019. The new ichthyosauriform *Chaohusaurus brevifemoralis* (Reptilia, Ichthyosauromorpha) from Majiashan, Chaohu, Anhui Province, China. *PeerJ* 7: e7561.

Hulke, J.W. 1873. Memorandum on some fossil vertebrate remains collected by the Swedish expeditions to Spitzbergen in 1864 and 1868. *Bihang Till Kongliga Svenska Vetenskaps-Akademiens Handlingar* 1 (9): 1–11

Hurum, J.H., Roberts, A.J., Nakrem, H.A., Stenløkk, J.A., and Mørk, A. 2014. The first recovered ichthyosaur from the Middle Triassic of Edgeøya, Svalbard. *Norwegian Petroleum Directorate Bulletin* 11: 97–110.

Ji, C., Jiang, D.-Y., Motani, R., Rieppel, O., Hao, W.-C., and Sun, Z.-Y. 2016. Phylogeny of the Ichthyopterygia incorporating recent discoveries from South China. *Journal of Vertebrate Paleontology* 36 (1): e1025956.

Jiang, D.-Y., Hao, W.-C., Maisch, M.W., Matzke, A.T., and Sun, Y.-L. 2005. A basal mixosaurid ichthyosaur from the Middle Triassic of China. *Palaeontology* 48: 869–882.

Jiang, D.-Y., Hao, W.-C., Motani, R., Schmitz, L., Sun, Y.-L., and Sun, Z.-Y. 2008a. Middle Triassic mixosaurids of Panxian, Guizhou and problems of "*Mixosaurus yangjuanensis* Liu and Yin, 2008" [in Chinese, with English abstract]. *Acta Palaeontologica Sinica* 47: 377–384.

Jiang, D.-Y., Hao, W.-C., Sun, Y.-L., Maisch, M.W., and Matzke, A.T. 2003. The mixosaurid ichthyosaur *Phalarodon* from the Middle Triassic of China. *Neues Jahrbuch für Geologie und Paläontologie, Monatshefte* 2003 (11): 656–666.

Jiang, D.-Y., Motani, R., Hao, W.-C., Rieppel, O., Sun, Y.-L., Schmitz, L., and Sun, Z.-Y. 2008b. First record of Placodontoidea (Reptilia, Sauropterygia, Placodontia) from the eastern Tethys. *Journal of Vertebrate Paleontology* 28: 904–908.

Jiang, D.-Y., Motani, R., Hao, W.-C., Rieppel, O., Sun, Y.-L., Tintori, A., Sun, Z.-Y., and Schmitz, L. 2009. Biodiversity and sequence of the Middle Triassic Panxian marine reptile fauna, Guizhou Province, China. *Acta Geologica Sinica, English Edition* 83: 451–459.

Jiang, D.-Y., Schmitz, L., Hao, W.-C., and Sun, Y.-L. 2006. A new mixosaurid ichthyosaur from the Middle Triassic of China. *Journal of Vertebrate Paleontology* 26: 60–69.

Jiang, D.-Y., Schmitz, L., Motani, R., Hao, W.-C., and Sun, Y.-L. 2007. The mixosaurid ichthyosaur *Phalarodon* cf. *P. fraasi* from the Middle Triassic of Guizhou Province, China. *Journal of Paleontology* 81: 602–605.

Kear, B.P., Engelschiøn, V.S., Hammer, Ø., Roberts, A.J., and Hurum, J.H. 2023. Earliest Triassic ichthyosaur fossils push back oceanic reptile origins. *Current Biology* 33 (5): R178–R179.

Kolb, C., Sánchez-Villagra, M.R., and Scheyer, T.M. 2011. The palaeohistology of the basal ichthyosaur *Mixosaurus* Baur, 1887 (Ichthyopterygia, Mixosauridae) from the Middle Triassic: Palaeobiological implications. *Comptes Rendus Palevol* 10: 403–411.

Li, Q. and Liu, J. 2020. An Early Triassic sauropterygian and associated fauna from South China provide insights into Triassic ecosystem health. *Communications Biology* 3: 63.

Liu, G.-B. and Yin, G.-Z. 2008. Preliminary researches for mixosaurid fossils from Middle Triassic Guanling Formation in Panxian of Guizhou [in Chinese, with English abstract]. *Acta Palaeontologica Sinica* 47: 73–90.

Liu, J. 2011. *Middle Triassic Mixosaurid Ichthyosaurs From SW China*. xxiii + 207 pp. The University of Hong Kong, Hong Kong.

Liu, J., Aitchison, J.C., Sun, Y.-Y., Zhang, Q.-Y., Zhou, C.-Y., and Lv, T. 2011. New mixosaurid ichthyosaur specimen from the middle Triassic of SW China: further evidence for the diapsid origin of ichthyosaurs. *Journal of Paleontology* 85: 32–36.

Liu, J. and Sander, P.M. 2019. The Vossenveld Formation and biotic recovery from the Permo-Triassic extinction. *Staringia* 16 (5–6): 147–152.

Liu, J., Hu, S.-X., Rieppel, O.C., Jiang, D.-Y., Benton, M.J., Kelley, N.P., Aitchison, J.C., Zhou, C.-Y., Wen, W., Huang, J.-Y., Xie, T., and Lv, T. 2014. A gigantic nothosaur (Reptilia: Sauropterygia) from the Middle Triassic of SW China and its implication for the Triassic biotic recovery. *Scientific Reports* 4: 7142.

Liu, J., Motani, R., Jiang, D.-Y., Hu, S.-X., Aitchison, J.C., Rieppel, O., Benton, M.J., Zhang, Q.-Y., and Zhou, C.-Y. 2013. The first specimen of the Middle Triassic *Phalarodon atavus* (Ichthyosauria: Mixosauridae) from South China, showing postcranial anatomy and peri-Tethyan distribution. *Palaeontology* 56: 849–866.

Lu, Y.-T. and Liu, J. 2023. A new tanystropheid (Diapsida: Archosauromorpha) from the Middle Triassic of SW China and the biogeographical origin of Tanystropheidae. *Journal of Systematic Palaeontology* 21 (1): 2250778.

Maddison, W.P. and Maddison, D.R. 2023. *Mesquite Project. Version 3.81. Mesquite: a Modular System for Evolutionary Analysis*. [downloaded from http://www.mesquiteproject.org/]

Maisch, M. 2010. Phylogeny, systematics, and origin of the Ichthyosauria—the state of the art. *Palaeodiversity* 3: 151–214.

Maisch, M.W. and Matzke, A.T. 1998a. Observations on Triassic ichthyosaurs. Part III: A crested predatory mixosaurid from the Middle Triassic of the Germanic Basin. *Neues Jahrbuch für Geologie und Paläontologie, Abhandlungen* 209: 105–134.

Maisch, M.W. and Matzke, A.T. 1998b. Observations on Triassic ichthyosaurs. Part IV: On the forelimb of *Mixosaurus* BAUR, 1887. *Neues Jahrbuch fur Geologie und Palaontologie, Abhandlungen* 209 (2): 247–272.

Maisch, M.W. and Matzke, A.T. 2000. The mixosaurid ichthyosaur *Contectopalatus* from the Middle Triassic of the German Basin. *Lethaia* 33: 71–74.

Maisch, M.W. and Matzke, A.T. 2001. The cranial osteology of the Middle Triassic ichthyosaur *Contectopalatus* from Germany. *Palaeontology* 44: 1127–1156.

Maisch, M.W., Matzke, A.T., and Brinkmann, W. 2006. The otic capsule of the Middle Triassic ichthyosaur. *Mixosaurus* from Monte San Giorgio (Switzerland): New evidence on the braincase structure of basal ichthyosaurs. *Eclogae Geologicae Helvetiae* 99: 205–210.

Maxwell, E.E. and Kear, B.P. 2013. Triassic ichthyopterygian assemblages of the Svalbard archipelago: a reassessment of taxonomy and distribution. *GFF* 135: 85–94.

Maxwell, E.E., Caldwell, M.W., and Lamoureux, D.O. 2012a. Tooth histology, attachment, and replacement in the Ichthyopterygia reviewed in an evolutionary context. *Paläontologische Zeitschrift* 86: 1–14.

Maxwell, E.E., Scheyer, T.M., and Fowler, D.A. 2014. An evolutionary and developmental perspective on the loss of regionalization in the limbs of derived ichthyosaurs. *Geological Magazine* 151: 29–40.

Maxwell, E.E., Zammit, M., and Druckenmiller, P.S. 2012b. Morphology and orientation of the ichthyosaurian femur. *Journal of Vertebrate Paleontology* 32: 1207–1211.

McGowan, C. and Motani, R. 2003. *Handbook of Palaeoherpetology. Part 8: Ichthyopterygia*. 175 pp. Verlag Dr. Friedrich Pfeil, München.

Merriam, J.C. 1910. The skull and dentition of a primitive ichthyosaurian from the Middle Triassic. *University of California Publications, Bulletin of the Department of Geology* 5 (24): 381–390.

Miedema, F., Bindellini, G., Dal Sasso, C., Scheyer, T.M., and Maxwell, E.E. 2023a. Ontogenetic variation in the cranium of *Mixosaurus cornalianus*, with implications for the evolution of ichthyosaurian cranial development. *Swiss Journal of Palaeontology* 142: 27.

Miedema, F., Klein, N., Blackburn, D.G., Sander, P.M., Maxwell, E.E., Griebeler, E.M., and Scheyer, T.M. 2023b. Heads or tails first? Evolution of fetal orientation in ichthyosaurs, with a scrutiny of the prevailing hypothesis. *BMC Ecology and Evolution* 23: 12.

Moon, B.C. 2019. A new phylogeny of ichthyosaurs (Reptilia: Diapsida). *Journal of Systematic Palaeontology* 17: 129–155.

Motani, R. 1997a. New information on the forefin of *Utatsusaurus hataii* (Ichthyosauria). *Journal of Paleontology* 71: 475–479.

Motani, R. 1997b. Temporal and spatial distribution of tooth implantations in ichthyosaurs. *In*: J.M. Callaway and E.L. Nicholls (eds.), *Ancient Marine Reptiles*, 81–103. Academic Press, San Diego.

Motani, R. 1998. First complete forefin of the ichthyosaur *Grippia longirostris* from the Triassic of Spitsbergen. *Palaeontology* 41: 591–599.

Motani, R. 1999a. On the evolution and homologies of ichthyopterygian forefins. *Journal of Vertebrate Paleontology* 19: 28–41.

Motani, R. 1999b. The skull and taxonomy of *Mixosaurus* (Ichthyopterygia). *Journal of Paleontology* 73: 924–935.

Motani, R. 2005a. Detailed tooth morphology in a durophagous ichthyosaur captured by 3D laser scanner. *Journal of Vertebrate Paleontology* 25: 462–465.

Motani, R. 2005b. Evolution of fish-shaped reptiles (Reptilia: Ichthyopterygia) in their physical environments and constraints. *Annual Review of Earth and Planetary Sciences* 33: 395–420.

Motani, R., Chen, X.-H., Jiang, D.-Y., Cheng, L., Tintori, A., and Rieppel, O. 2015. Lunge feeding in early marine reptiles and fast evolution of marine tetrapod feeding guilds. *Scientific Reports* 5: 8900.

Motani, R., Jiang, D.-Y., Tintori, A., Ji, C., and Huang, J.-D. 2017. Pre-versus post-mass extinction divergence of Mesozoic marine reptiles dictated by time-scale dependence of evolutionary rates. *Proceedings of the Royal Society B: Biological Sciences* 284: 1–8.

Motani, R., Jiang, D.-Y., Tintori, A., Sun, Y.-L., Hao, W.-C., Boyd, A., Hinic-Frlog, S., Schmitz, L., Shin, J.-Y., and Sun, Z.-Y. 2008. Horizons and assemblages of Middle Triassic marine reptiles from Panxian, Guizhou, China. *Journal of Vertebrate Paleontology* 28: 900–903.

Motani, R., You, H., and McGowan, C. 1996. Eel-like swimming in the earliest ichthyosaurs. *Nature* 382: 347–348.

Nicholls, E.L., Brinkman, D.B., and Callaway, J.M. 1999. New material of *Phalarodon* (Reptilia: Ichthyosauria) from the Triassic of British Columbia and its bearing on the interrelationships of mixosaurs. *Palaeontographica, Abteilung A: Palaozoologie, Stratigraphie* 252 (1–3): 1–22.

Økland, I.H., Delsett, L.L., Roberts, A.J., and Hurum, J.H. 2018. A *Phalarodon fraasi* (Ichthyosauria: Mixosauridae) from the Middle Triassic of Svalbard. *Norwegian Journal of Geology* 98: 267–288.

Pol, D. and Escapa, I.H. 2009. Unstable taxa in cladistic analysis: Identification and the assessment of relevant characters. *Cladistics* 25: 515–527.

Qiao, Y., Liu, J., Wolniewicz, A.S., Iijima, M., Shen, Y.-F., Wintrich, T., Li, Q., and Sander, P.M. 2022. A globally distributed durophagous marine reptile clade supports the rapid recovery of pelagic ecosystems after the Permo-Triassic mass extinction. *Communications Biology* 5: 1242.

Quenstedt, F.A. 1852. *Handbuch der Petrefaktenkunde*. iv + 792 pp. H. Laupp, Tübingen.

Renesto, S., Dal Sasso, C., Fogliazza, F., and Ragni, C. 2020. New findings reveal that the Middle Triassic ichthyosaur *Mixosaurus cornalianus* is the oldest amniote with a dorsal fin. *Acta Palaeontologica Polonica* 65: 511–522.

Repossi, E. 1902. Il Mixosauro degli strati Triasici di Besano in Lombardia. *Atti della Società italiana di scienze naturali e del Museo civico di storia naturale di Milano* 41: 361–372.

Roberts, A.J., Engelschiøn, V.S., and Hurum, J.H. 2022. First three-dimensional skull of the Middle Triassic mixosaurid ichthyosaur *Phalarodon fraasi* from Svalbard, Norway. *Acta Palaeontologica Polonica* 67: 51–62.

Sander, P.M. and Mazin, J.-M. 1993. The paleobiogeography of Middle Triassic ichthyosaurs: The five major faunas. *Paleontologia Lombarda, Nuova Serie* 2: 145–152.

Sander, P.M., Griebeler, E.M., Klein, N., Juarbe, J.V., Wintrich, T., Revell, L.J., and Schmitz, L. 2021. Early giant reveals faster evolution of large body size in ichthyosaurs than in cetaceans. *Science* 374: eabf5787.

Scheyer, T.M., Romano, C., Jenks, J., and Bucher, H. 2014. Early Triassic Marine Biotic Recovery: The Predators' Perspective. *PLoS ONE* 9 (3): e88987.

Schmitz, L. 2005. The taxonomic status of *Mixosaurus nordenskioeldii* (Ichthyosauria). *Journal of Vertebrate Paleontology* 25: 983–985.

Schmitz, L., Sander, P.M., Storrs, G.W., and Rieppel, O. 2004. New Mixosauridae (Ichthyosauria) from the Middle Triassic of the Augusta Mountains (Nevada, USA) and their implications for mixosaur taxonomy. *Palaeontographica, Abteilung A: Palaozoologie, Stratigraphie* 270 (4–6): 133–162.

Song, H.-J., Wignall, P.B., and Dunhill, A.M. 2018. Decoupled taxonomic and ecological recoveries from the Permo-Triassic extinction. *Science Advances* 4 (10): 1–7.

Tintori, A., Lombardo, C., and Sun, Z. 2017. Triassic actinopterygians across Tethys: state of the art. *Research & Knowledge* 3 (2): 65–68.

Wen, W., Zhang, Q.-Y., Hu, S.-X., Zhou, C.-Y., Huang, J.-Y., Ma, Z.-X., and Min, X. 2020. New occurrence and significance of Middle Triassic Luoping Biota from Luxi County, Yunnan Province [in Chinese, with English abstract]. *Earth Science-Journal of China University of Geo-Sciences* 45 (8): 3094–3103.

Xiong, Z.-F. 2020. *Two New Specimens of Middle Triassic Mixosaurid Ichthyosaurs from Yunnan and Guizhou, China* [in Chinese, with English abstract]. viii + 87 pp. Hefei University of Technology, Hefei.

Xu, G.-H., Ren, Y., Zhao, L.-J., Liao, J.-L., and Feng, D.-H. 2022. A long-tailed marine reptile from China provides new insights into the Middle Triassic pachypleurosaur radiation. *Scientific Reports* 12 (1): 7396.

Yin, G.-Z., Zhou, X.-G., Cao, Z.-T., Yu, Y.-Y., and Luo, Y.-M. 2000. A preliminary study on the Early Late Triassic marine reptiles from Guanling, Guizhou, China [in Chinese, with English abstract]. *Geology, Geochemistry* 28 (3): 1–23.

Young, C.-C. 1965. On a revised determination of a fossil reptile from Jenhui, Kweichou with note on a new ichthyosaur probably from China [in Chinese, with English abstract]. *Vertebrata PalAsiatica* 9 (4): 368–375.

Zang, Z. 2014. *Morphological Study on a* Mixosaurus panxianensis *from the Middle Triassic of Panxian, Guizhou*. 43 pp. [in Chinese, with English abstract]. Shandong University of Science and Technology, Qingdao.

Zhou, M., Jiang, D.-Y., Motani, R., and Lu, H. 2022. The morphological differences and intraspecific variation of the forefins of *Mixosaurus panxianensis* from Panzhou, Guizhou [in Chinese, with English abstract]. *Acta Palaeontologica Sinica* 61: 643–653.